Collider Phenomenology

— From basic knowledge to new physics searches

Tao Han

University of Wisconsin – Madison

BUSSTEPP 2010

Univ. of Swansea, Aug. 23–Sept. 3, 2010

Outline:

Lecture I: Colliders and Detectors

Outline:

Lecture I: Colliders and Detectors

Lecture II: Basics Techniques and Tools

Outline:

Lecture I: Colliders and Detectors

Lecture II: Basics Techniques and Tools

Lecture III: (a). An e^+e^- Linear Collider

(b). Perturbative QCD at Hadron Colliders

(c). Hadron Colliders Physics

Outline:

Lecture I: Colliders and Detectors

Lecture II: Basics Techniques and Tools

Lecture III: (a). An e^+e^- Linear Collider

(b). Perturbative QCD at Hadron Colliders

(c). Hadron Colliders Physics

Lecture IV: From Kinematics to Dynamics

Outline:

Lecture I: Colliders and Detectors

Lecture II: Basics Techniques and Tools

Lecture III: (a). An e^+e^- Linear Collider

(b). Perturbative QCD at Hadron Colliders

(c). Hadron Colliders Physics

Lecture IV: From Kinematics to Dynamics

Lecture V: Search for New Physics at Hadron Colliders

Outline:

Lecture I: Colliders and Detectors

Lecture II: Basics Techniques and Tools

Lecture III: (a). An e^+e^- Linear Collider

(b). Perturbative QCD at Hadron Colliders

(c). Hadron Colliders Physics

Lecture IV: From Kinematics to Dynamics

Lecture V: Search for New Physics at Hadron Colliders

Main reference: TASI 04 Lecture notes
hep-ph/0508097,
plus the other related lectures in this school.

Opening Remarks: LHC is in mission!

Opening Remarks: LHC is in mission!

Running at $E_{cm} = 3.5 \oplus 3.5$ TeV,

he collider and detecters are all performing well!
New era in HEP and in science has just begun!

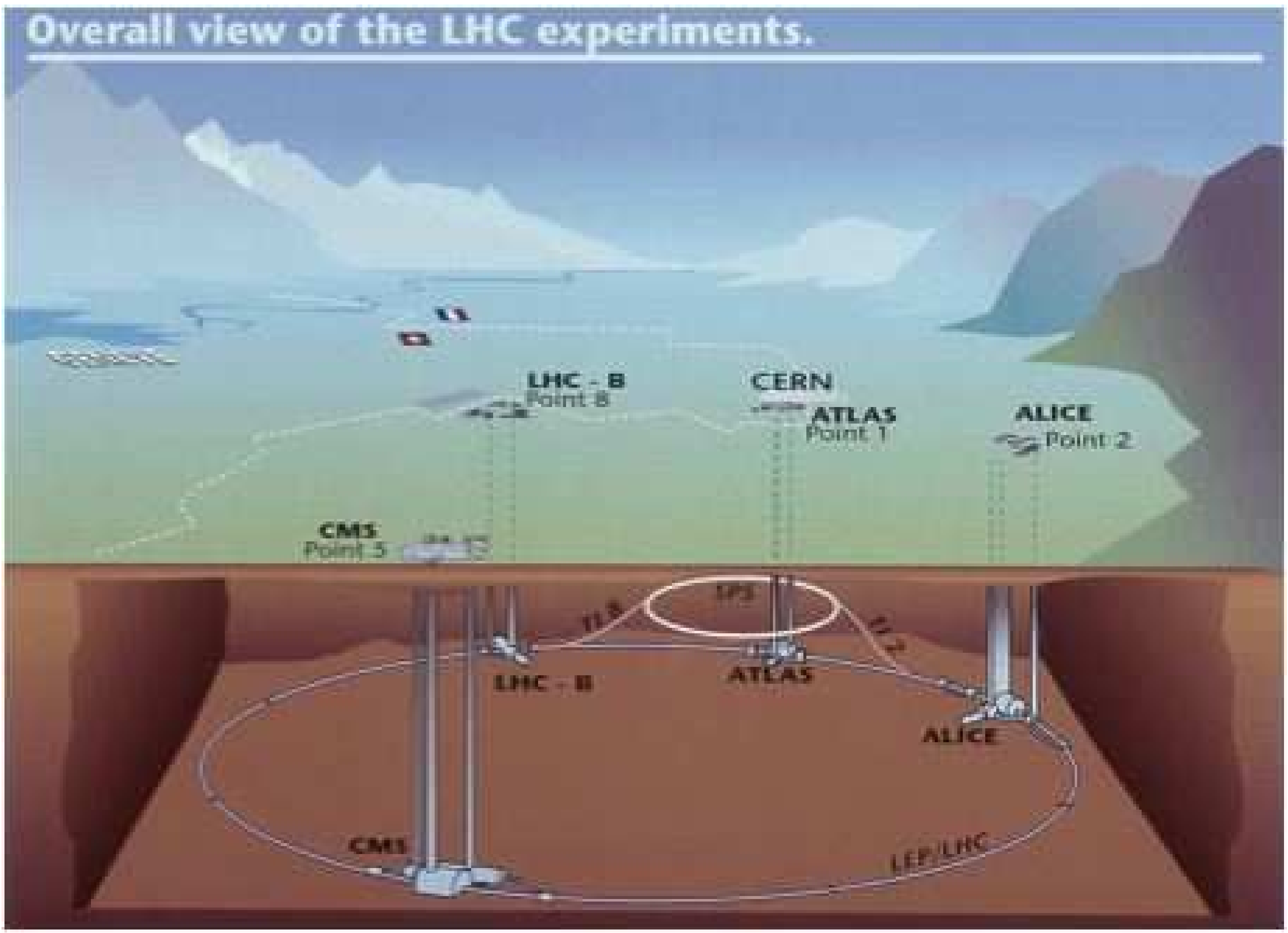

SM particles have been re-discovered!

SM particles have been re-discovered!

EW gauge bosons:

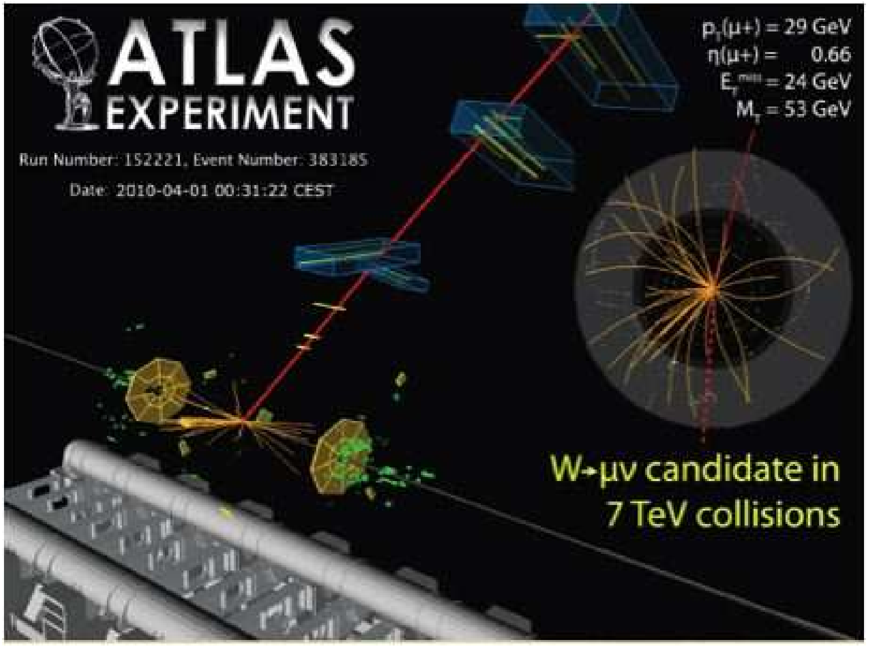

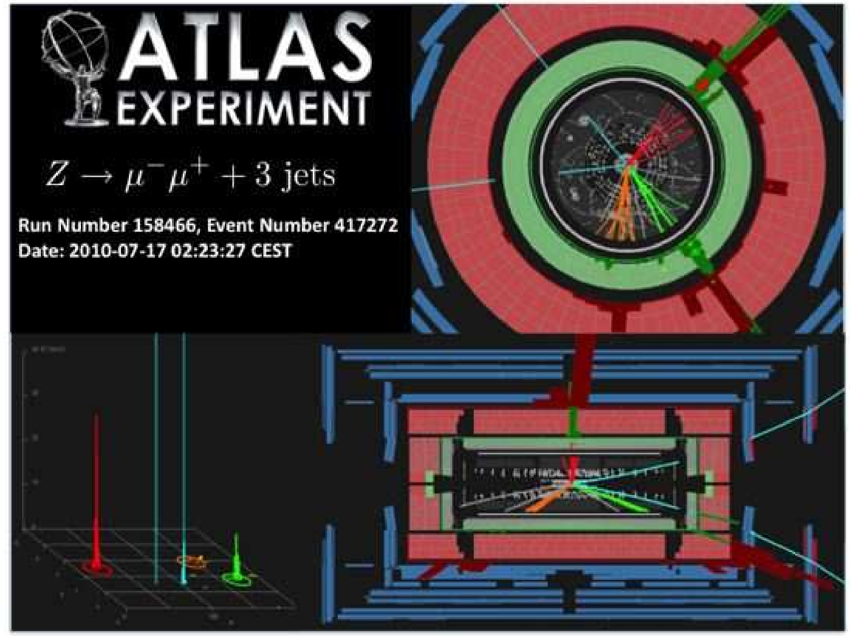

SM particles have been re-discovered!

EW gauge bosons:

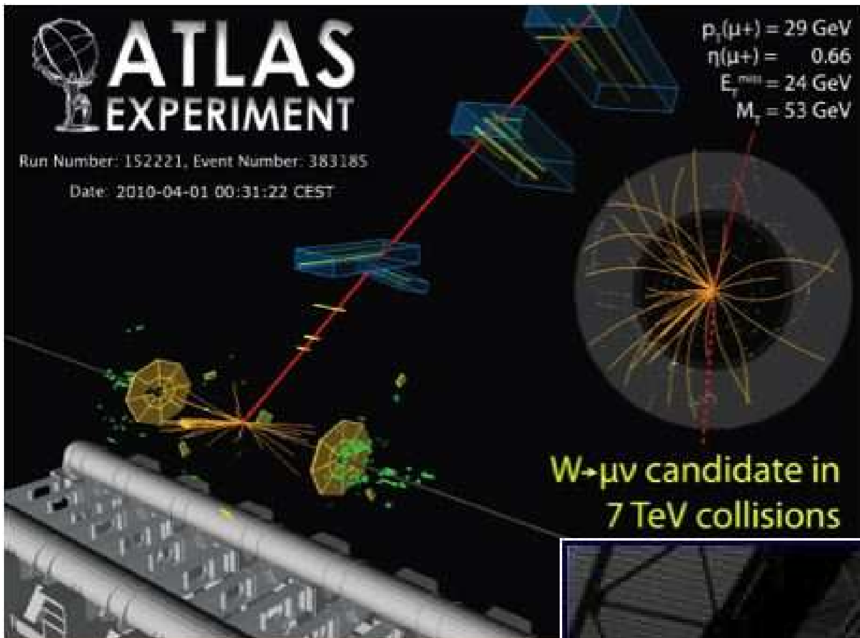

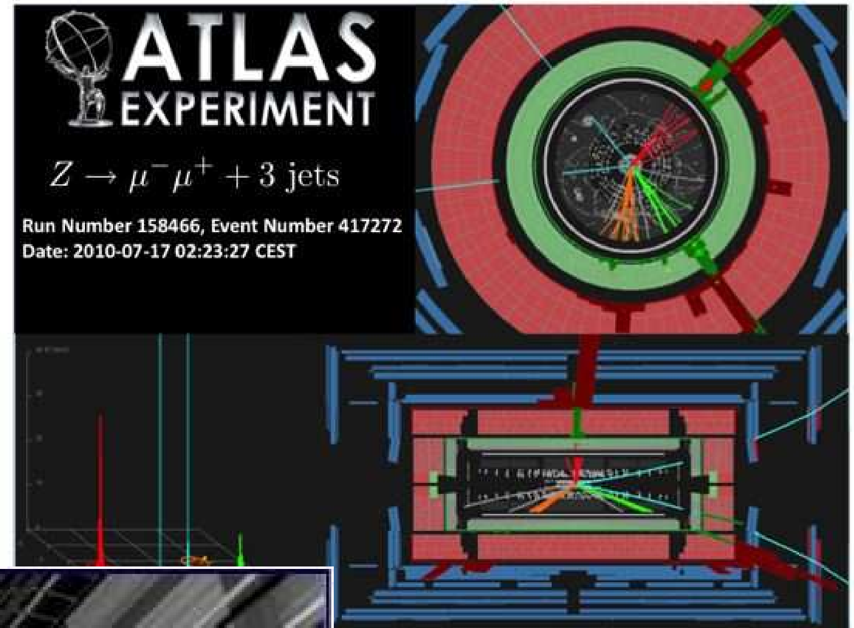

Heavy quarks:

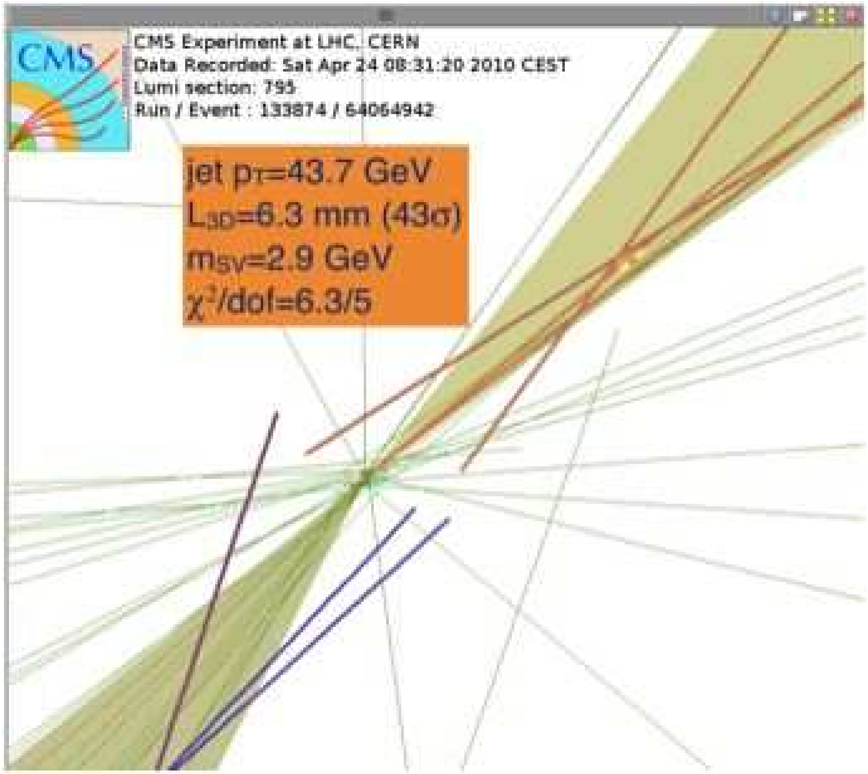

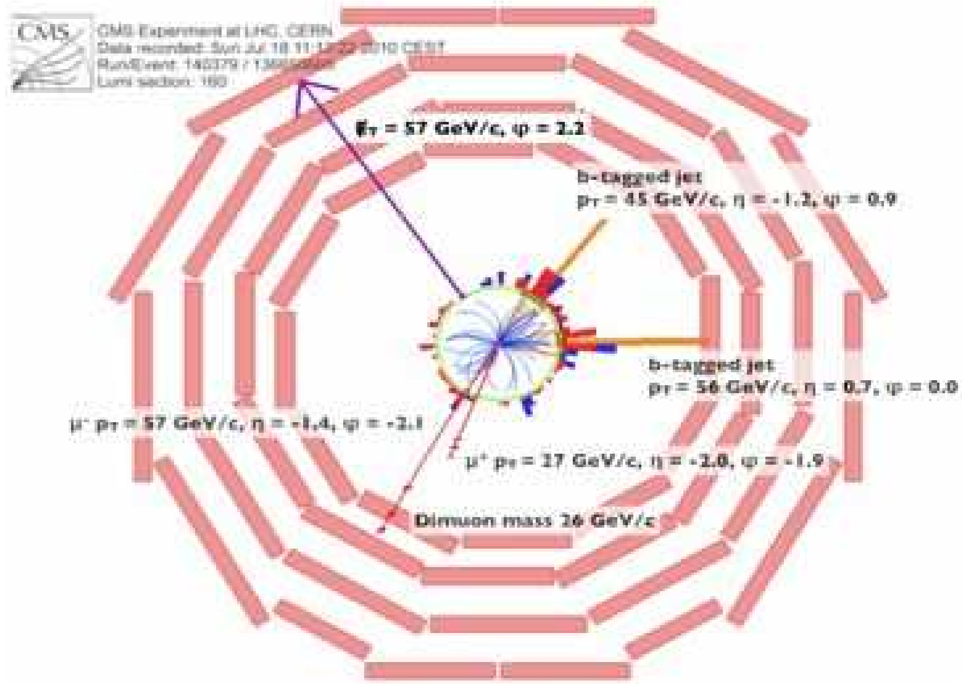

Heavy quarks:

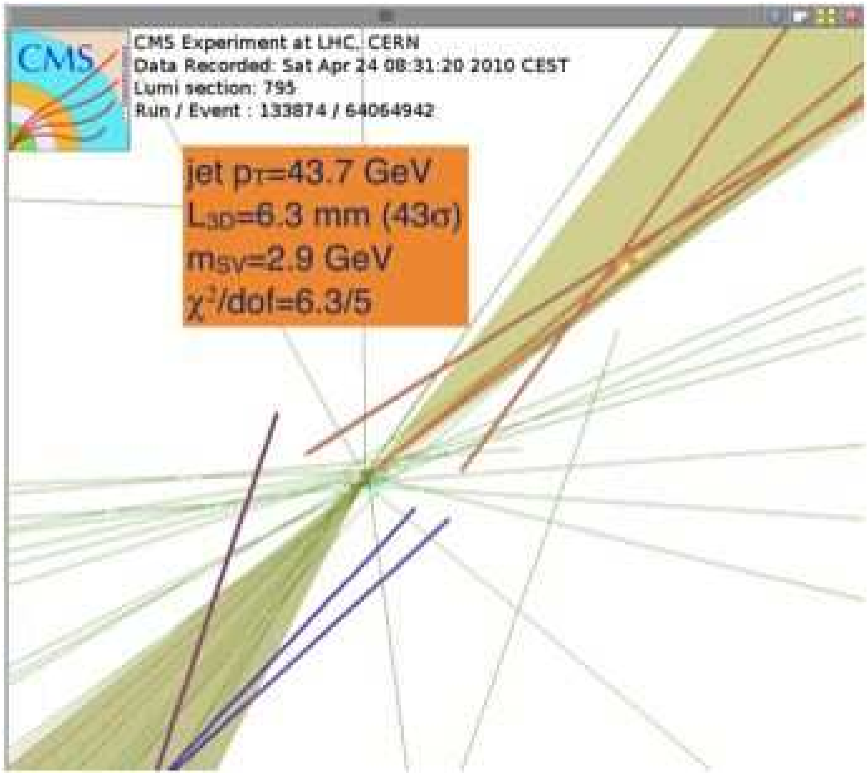

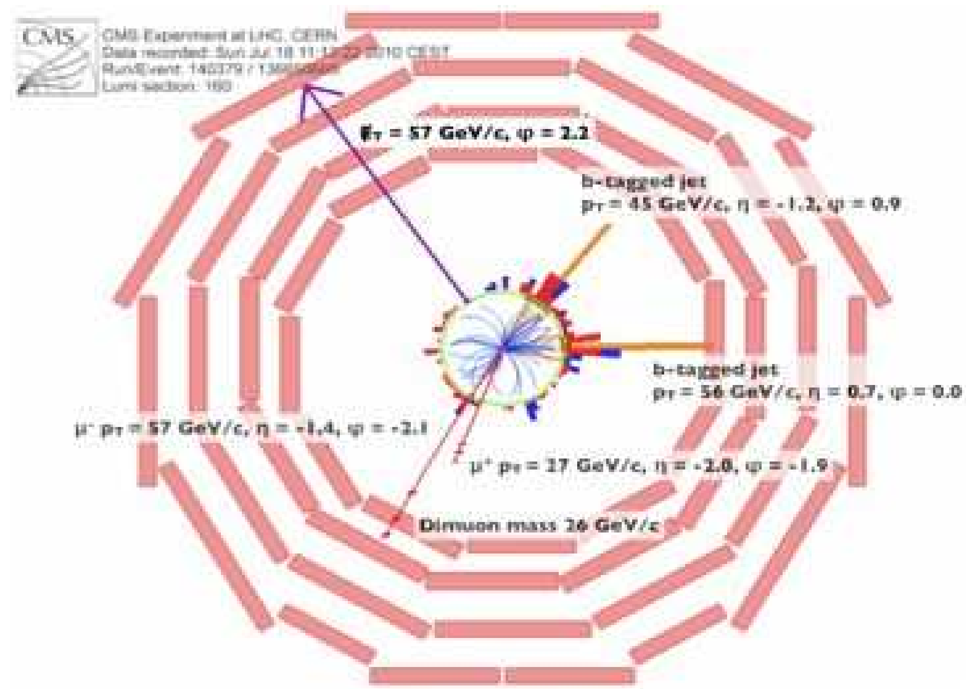

We are ready for new discoveries !

I. Colliders and Detectors

(A). High-energy Colliders:

To study the deepest layers of matter,

we need the probes with highest energies.

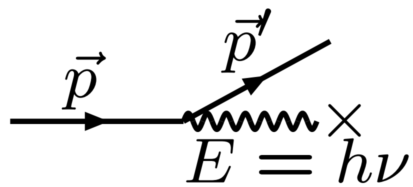

I. Colliders and Detectors

(A). High-energy Colliders:

To study the deepest layers of matter,
we need the probes with highest energies.

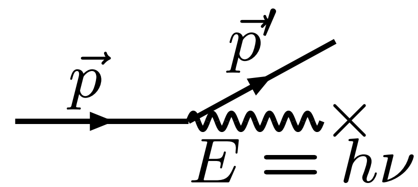

Two parameters of importance:

1. The energy:

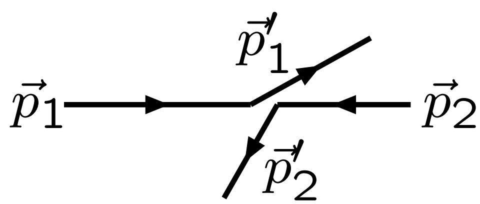

$$s \equiv (p_1 + p_2)^2 = \begin{cases} (E_1 + E_2)^2 - (\vec{p}_1 + \vec{p}_2)^2, \\ m_1^2 + m_2^2 + 2(E_1 E_2 - \vec{p}_1 \cdot \vec{p}_2). \end{cases}$$

$$E_{cm} \equiv \sqrt{s} \approx \begin{cases} 2E_1 \approx 2E_2 & \text{in the c.m. frame } \vec{p}_1 + \vec{p}_2 = 0, \\ \sqrt{2E_1 m_2} & \text{in the fixed target frame } \vec{p}_2 = 0. \end{cases}$$

2. The luminosity:

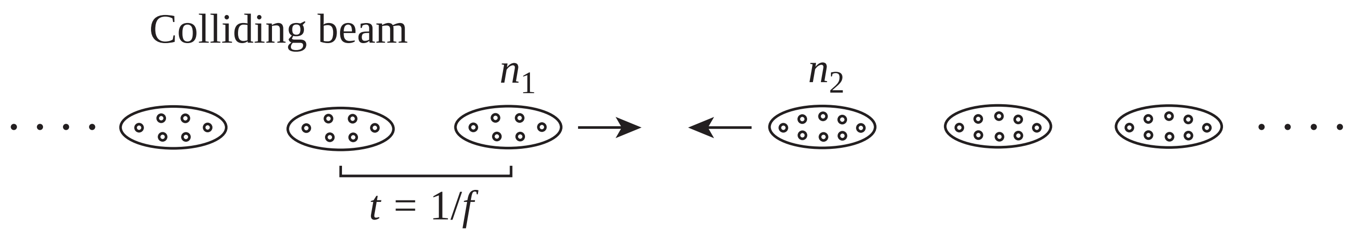

$$\mathcal{L} \propto f n_1 n_2 / a,$$

(a some beam transverse profile) in units of #particles/cm^2/s

$\Rightarrow 10^{33}$ cm^{-2}s $^{-1}$ $=$ 1 nb^{-1} s^{-1} $\approx$ 10 fb^{-1}/year.

2. The luminosity:

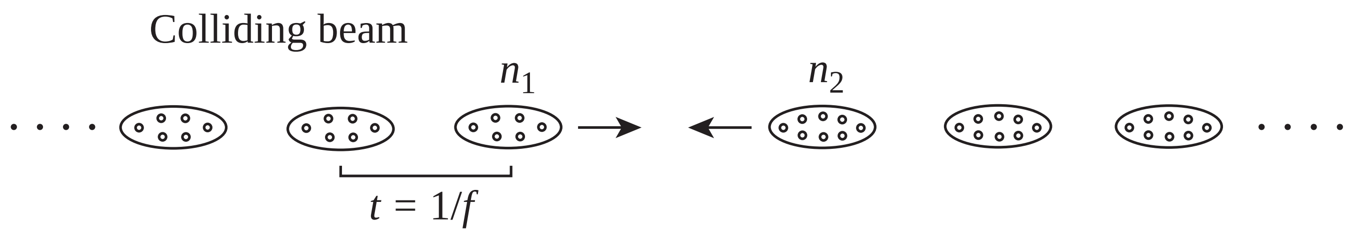

$$\mathcal{L} \propto f n_1 n_2 / a,$$

(a some beam transverse profile) in units of #particles/cm^2/s

$\Rightarrow 10^{33}\ \text{cm}^{-2}\text{s}^{-1} = 1\ \text{nb}^{-1}\ \text{s}^{-1} \approx 10\ \ \text{fb}^{-1}/\text{year}.$

Current and future high-energy colliders:

Hadron Colliders	$\sqrt{s}$ (TeV)	$\mathcal{L}$ (cm^{-2}s^{-1})	$\delta E/E$	f (MHz)	#/bunch (10^{10})	L (km)
Tevatron	1.96	2.1×10^{32}	9×10^{-5}	2.5	p: 27, $\bar{p}$: 7.5	6.28
LHC	(7) 14	(10^{32}) 10^{34}	0.01%	40	10.5	26.66

2. The luminosity:

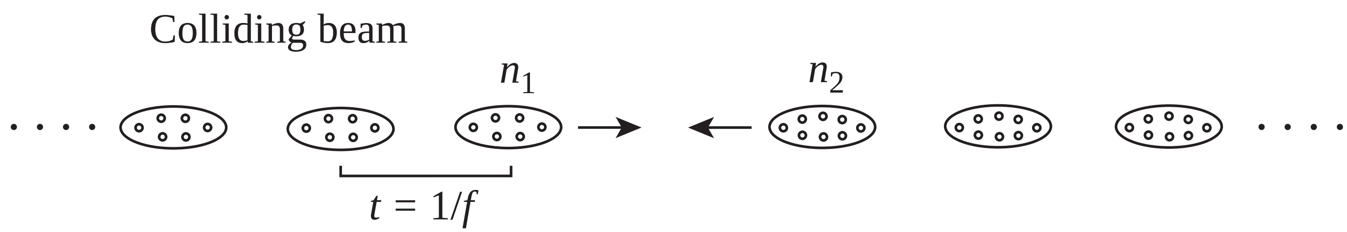

$$\mathcal{L} \propto f n_1 n_2 / a,$$

(a some beam transverse profile) in units of #particles/cm^2/s

$\Rightarrow 10^{33}\ \text{cm}^{-2}\text{s}^{-1} = 1\ \text{nb}^{-1}\ \text{s}^{-1} \approx 10\ \text{fb}^{-1}/\text{year}.$

Current and future high-energy colliders:

Hadron Colliders	$\sqrt{s}$ (TeV)	$\mathcal{L}$ (cm^{-2}s^{-1})	$\delta E/E$	f (MHz)	#/bunch (10^{10})	L (km)
Tevatron	1.96	2.1×10^{32}	9×10^{-5}	2.5	p: 27, $\bar{p}$: 7.5	6.28
LHC	(7) 14	(10^{32}) 10^{34}	0.01%	40	10.5	26.66

e^+e^- Colliders	$\sqrt{s}$ (TeV)	$\mathcal{L}$ (cm^{-2}s^{-1})	$\delta E/E$	f (MHz)	polar.	L (km)
ILC	0.5–1	2.5×10^{34}	0.1%	3	80, 60%	14 – 33
CLIC	3–5	$\sim 10^{35}$	0.35%	1500	80, 60%	33 – 53

(B). An e^+e^- Linear Collider

The collisions between e^- and e^+ have major advantages:

- The system of an electron and a positron has zero charge, zero lepton number etc.,

$\Longrightarrow$ it is suitable to create new particles after e^+e^- annihilation.

- With symmetric beams between the electrons and positrons, the laboratory frame is the same as the c.m. frame,

$\Longrightarrow$ the total c.m. energy is fully exploited to reach the highest possible physics threshold.

(B). An e^+e^- Linear Collider

The collisions between e^- and e^+ have major advantages:

- The system of an electron and a positron has zero charge, zero lepton number etc.,

$\Longrightarrow$ it is suitable to create new particles after e^+e^- annihilation.

- With symmetric beams between the electrons and positrons, the laboratory frame is the same as the c.m. frame,

$\Longrightarrow$ the total c.m. energy is fully exploited to reach the highest possible physics threshold.

- With well-understood beam properties,

$\Longrightarrow$ the scattering kinematics is well-constrained.

- Backgrounds low and well-undercontrol.
- It is possible to achieve high degrees of beam polarizations,

$\Longrightarrow$ chiral couplings and other asymmetries can be effectively explored.

Disadvantages

- Large synchrotron radiation due to acceleration,

$$\Delta E \sim \frac{1}{R} \left(\frac{E}{m_e}\right)^4 .$$

Thus, a multi-hundred GeV e^+e^- collider will have to be made a linear accelerator.

- This becomes a major challenge for achieving a high luminosity when a storage ring is not utilized;
beamsstrahlung severe.

(C). Hadron Colliders

LHC: the new high-energy frontier

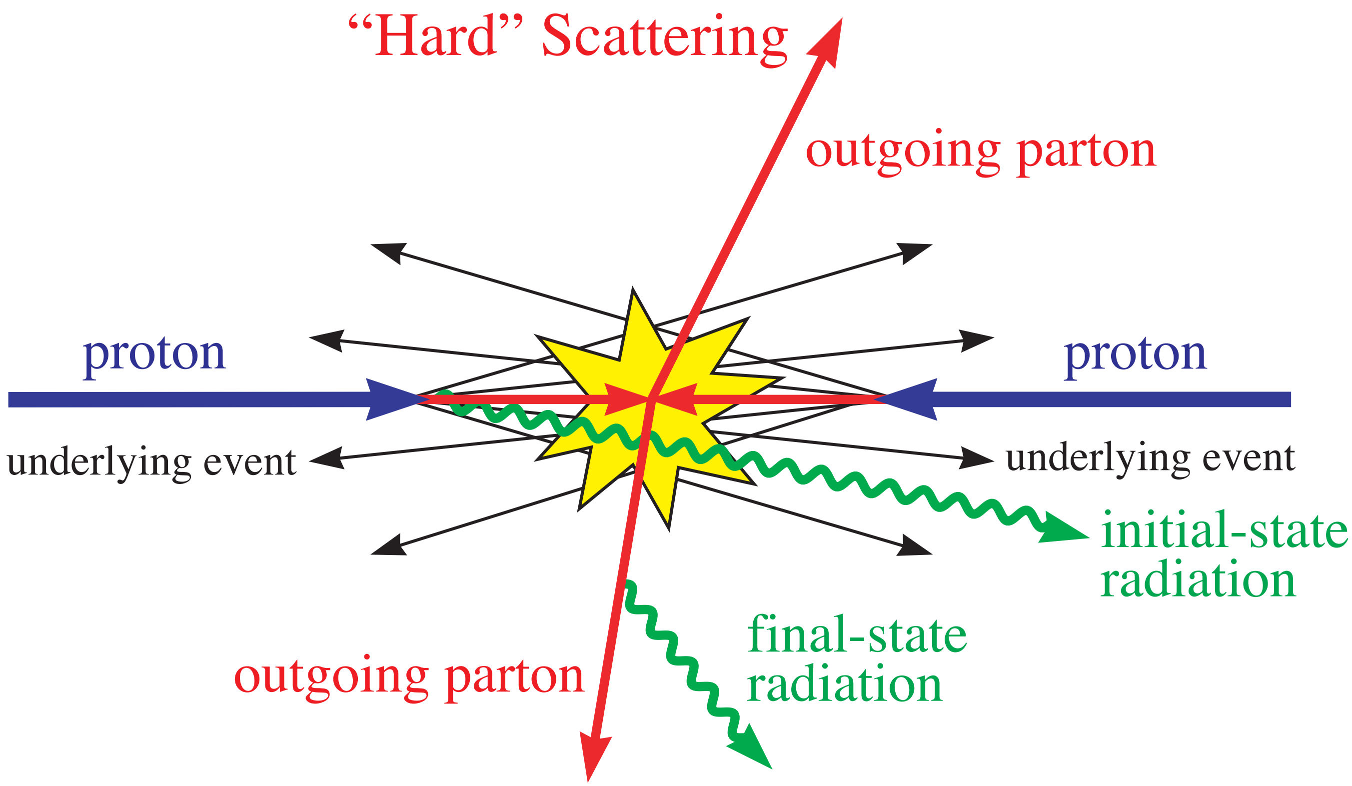

(C). Hadron Colliders

LHC: the new high-energy frontier

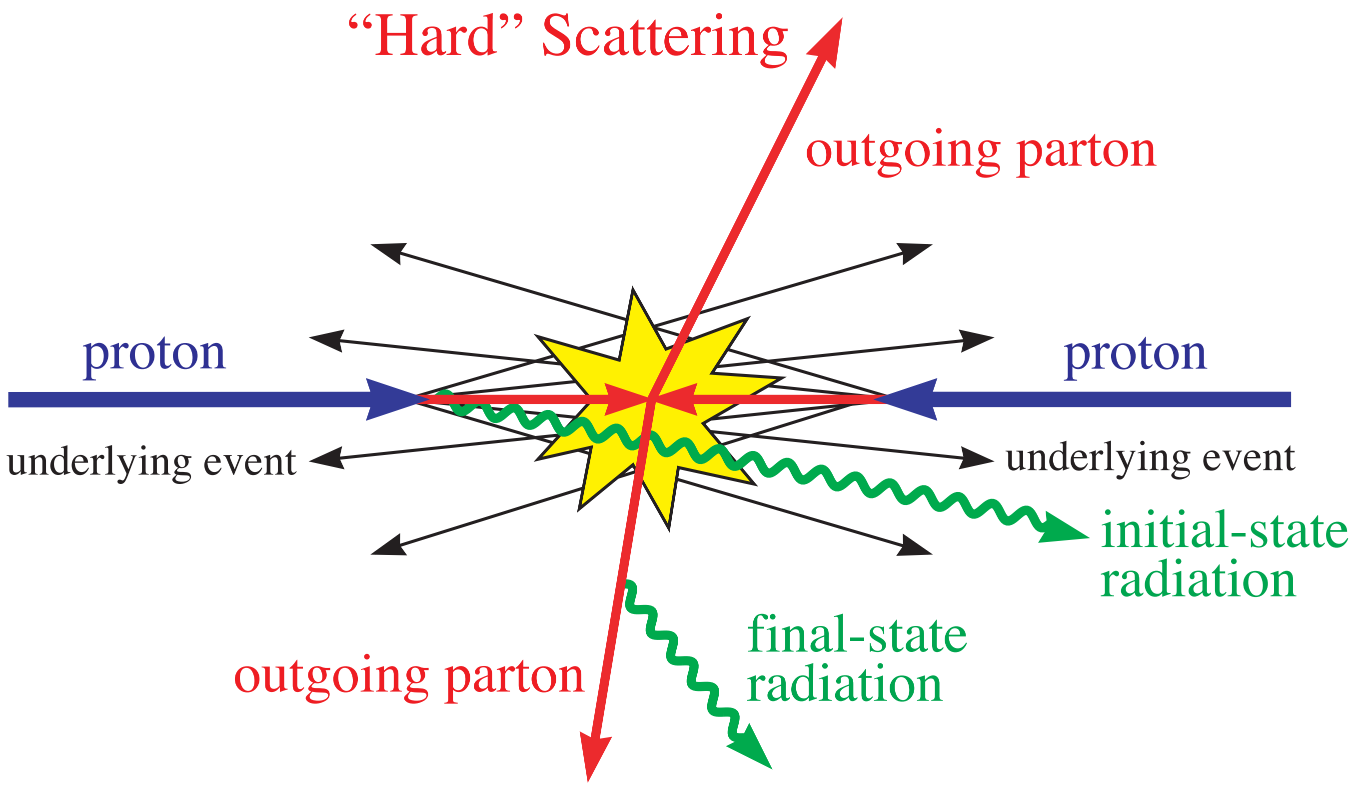

Advantages

• Higher c.m. energy, thus higher energy threshold:

$\sqrt{S} = 14$ TeV: $\quad M_{new}^2 \sim s = x_1 x_2 S \quad \Rightarrow \quad M_{new} \sim 0.2\sqrt{S} \sim 3$ TeV.

- Higher luminosity: 10^{34}/cm^2/s $\Rightarrow$ 100 fb^{-1}/yr.

    Annual yield: 1B $W^{\pm}$; 100M $t\bar{t}$; 10M $W^{+}W^{-}$; 1M H^{0}...

- Higher luminosity: 10^{34}/cm^2/s $\Rightarrow$ 100 fb^{-1}/yr.
  Annual yield: 1B $W^\pm$; 100M $t\bar{t}$; 10M W^+W^-; 1M H^0...
- Multiple (strong, electroweak) channels:
  $q\bar{q}'$, gg, qg, $b\bar{b} \to$ colored; $Q = 0, \pm 1$; $J = 0, 1, 2$ states;
  WW, WZ, ZZ, $\gamma\gamma \to I_W = 0, 1, 2$; $Q = 0, \pm 1, \pm 2$; $J = 0, 1, 2$ states.

- Higher luminosity: 10^{34}/cm^2/s $\Rightarrow$ 100 fb^{-1}/yr.
  Annual yield: 1B $W^{\pm}$; 100M $t\bar{t}$; 10M W^+W^-; 1M H^0...
- Multiple (strong, electroweak) channels:
  $q\bar{q}'$, gg, qg, $b\bar{b} \to$ colored; $Q = 0, \pm 1$; $J = 0, 1, 2$ states;
  WW, WZ, ZZ, $\gamma\gamma \to I_W = 0, 1, 2$; $Q = 0, \pm 1, \pm 2$; $J = 0, 1, 2$ states.

Disadvantages

- Initial state unknown:
  colliding partons unknown on event-by-event basis;
  parton c.m. energy unknown: $E_{cm}^2 \equiv s = x_1 x_2 S$;
  parton c.m. frame unknown.
  $\Rightarrow$ largely rely on final state reconstruction.

- Higher luminosity: 10^{34}/cm^2/s $\Rightarrow$ 100 fb^{-1}/yr.

  Annual yield: 1B $W^\pm$; 100M $t\bar{t}$; 10M W^+W^-; 1M H^0...
- Multiple (strong, electroweak) channels:

  $q\bar{q}'$, gg, qg, $b\bar{b} \rightarrow$ colored; $Q = 0, \pm 1$; $J = 0, 1, 2$ states;

  WW, WZ, ZZ, $\gamma\gamma \rightarrow I_W = 0, 1, 2$; $Q = 0, \pm 1, \pm 2$; $J = 0, 1, 2$ states.

Disadvantages

- Initial state unknown:

  colliding partons unknown on event-by-event basis;

  parton c.m. energy unknown: $E^2_{cm} \equiv s = x_1 x_2 S$;

  parton c.m. frame unknown.

  $\Rightarrow$ largely rely on final state reconstruction.
- The large rate turns to a hostile environment:

  $\Rightarrow$ Severe backgrounds!

- Higher luminosity: 10^{34}/cm^2/s $\Rightarrow$ 100 fb^{-1}/yr.

  Annual yield: 1B $W^{\pm}$; 100M $t\bar{t}$; 10M W^+W^-; 1M H^0...
- Multiple (strong, electroweak) channels:

  $q\bar{q}'$, gg, qg, $b\bar{b} \to$ colored; $Q = 0, \pm 1$; $J = 0, 1, 2$ states;

  WW, WZ, ZZ, $\gamma\gamma \to I_W = 0, 1, 2$; $Q = 0, \pm 1, \pm 2$; $J = 0, 1, 2$ states.

Disadvantages

- Initial state unknown:

  colliding partons unknown on event-by-event basis;

  parton c.m. energy unknown: $E_{cm}^2 \equiv s = x_1 x_2 S$;

  parton c.m. frame unknown.

  $\Rightarrow$ largely rely on final state reconstruction.
- The large rate turns to a hostile environment:

  $\Rightarrow$ Severe backgrounds!

Our primary job !

- *Path of the high-energy colliders:*

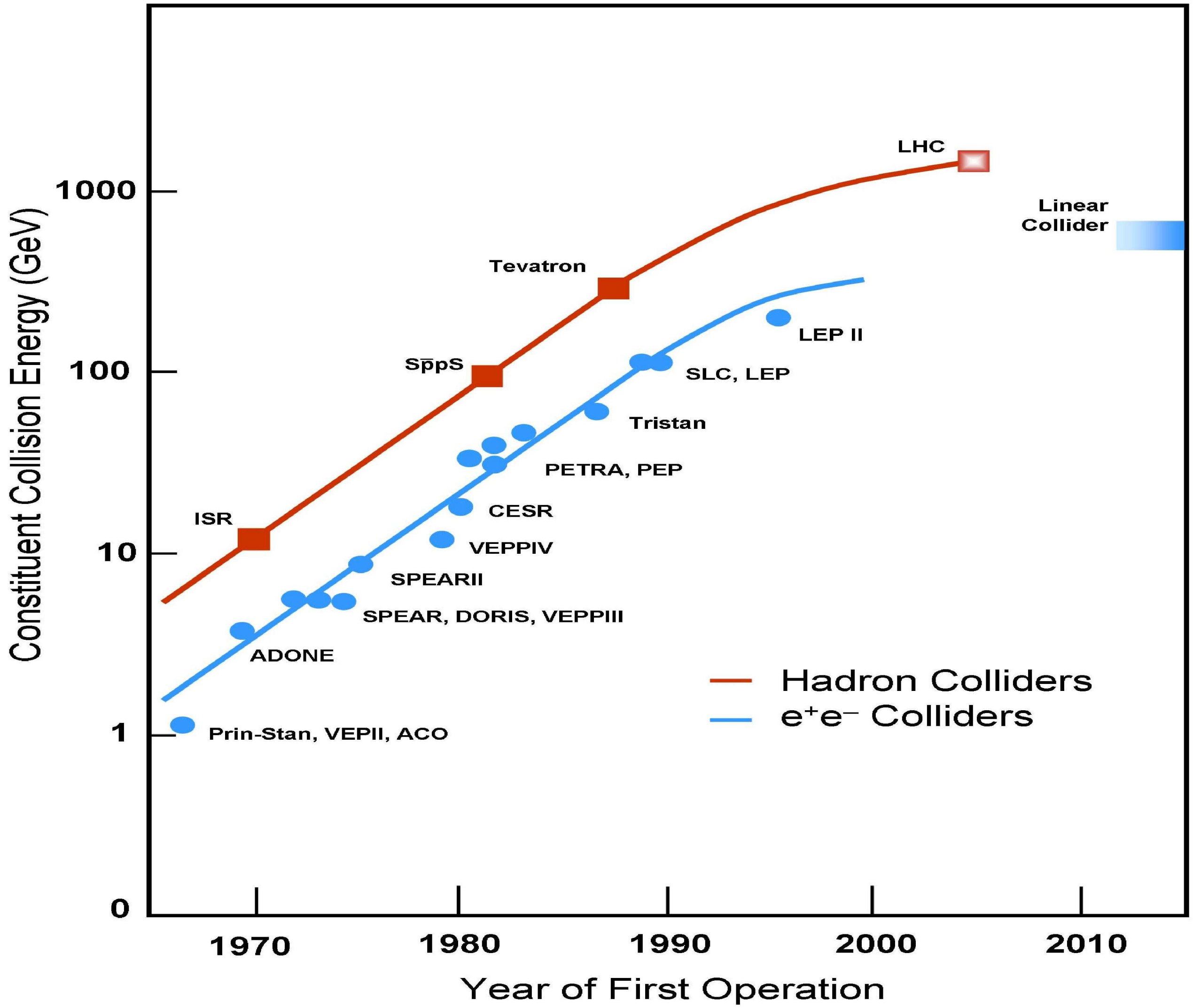

The LHC opens up a new eta of HEP for the decades to come.

(D). Particle Detection:

The detector complex:
Utilize the strong and electromagnetic interactions
between detector materials and produced particles.

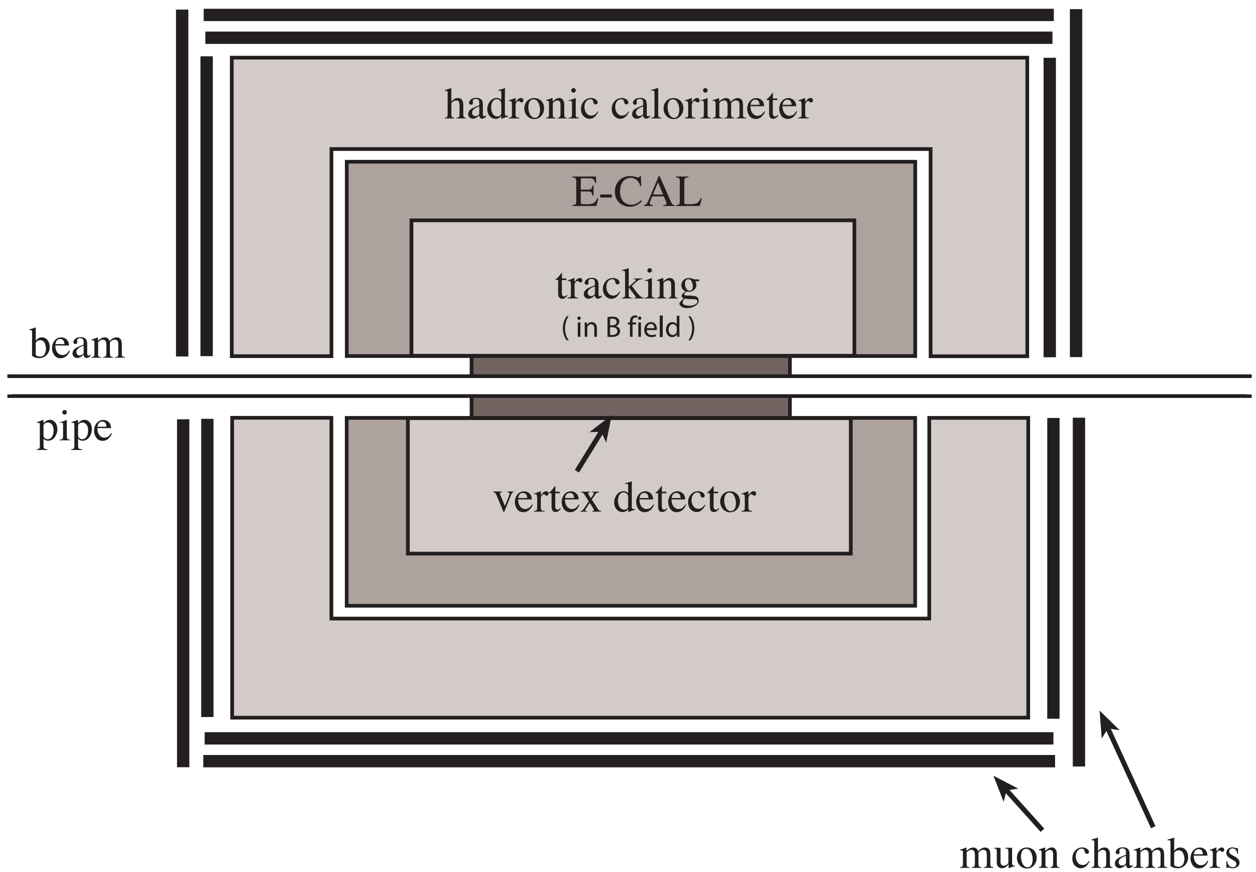

What we "see" as particles in the detector: (a few meters)

For a relativistic particle, the travel distance:

$$d = (\beta c\ \tau)\gamma \approx (300\ \mu m)(\frac{\tau}{10^{-12}\ s})\ \gamma$$

What we "see" as particles in the detector: (a few meters)

For a relativistic particle, the travel distance:

$$d = (\beta c\ \tau)\gamma \approx (300\ \mu m)(\frac{\tau}{10^{-12}\ s})\ \gamma$$

- stable particles directly "seen":

$$p,\ \bar{p},\ e^{\pm},\ \gamma$$

- quasi-stable particles of a life-time $\tau \geq 10^{-10}$ s also directly "seen":

$$n, \Lambda, K_L^0, ...,\ \mu^{\pm},\ \pi^{\pm}, K^{\pm}...$$

What we "see" as particles in the detector: (a few meters)

For a relativistic particle, the travel distance:

$$d = (\beta c\ \tau)\gamma \approx (300\ \mu m)(\frac{\tau}{10^{-12}\ s})\ \gamma$$

- stable particles directly "seen":

$$p,\ \bar{p},\ e^{\pm},\ \gamma$$

- quasi-stable particles of a life-time $\tau \geq 10^{-10}$ s also directly "seen":

$$n, \Lambda, K_L^0, ...,\ \mu^{\pm},\ \pi^{\pm}, K^{\pm}...$$

- a life-time $\tau \sim 10^{-12}$ s may display a secondary decay vertex, "vertex-tagged particles":

$$B^{0,\pm},\ D^{0,\pm},\ \tau^{\pm}...$$

What we "see" as particles in the detector: (a few meters)

For a relativistic particle, the travel distance:

$$d = (\beta c\ \tau)\gamma \approx (300\ \mu m)(\frac{\tau}{10^{-12}\ s})\ \gamma$$

- stable particles directly "seen":

$$p,\ \bar{p},\ e^{\pm},\ \gamma$$

- quasi-stable particles of a life-time $\tau \geq 10^{-10}$ s also directly "seen":

$$n, \Lambda, K_L^0, ...,\ \mu^{\pm},\ \pi^{\pm}, K^{\pm}...$$

- a life-time $\tau \sim 10^{-12}$ s may display a secondary decay vertex, "vertex-tagged particles":

$$B^{0,\pm},\ D^{0,\pm},\ \tau^{\pm}...$$

- short-lived not "directly seen", but "reconstructable":

$$\pi^0,\ \rho^{0,\pm}...\ ,\quad Z, W^{\pm}, t, H...$$

- missing particles are weakly-interacting and neutral:

$$\nu,\ \tilde{\chi}^0, G_{KK}...$$

† For stable and quasi-stable particles of a life-time $\tau \geq 10^{-10} - 10^{-12}$ s, they show up as

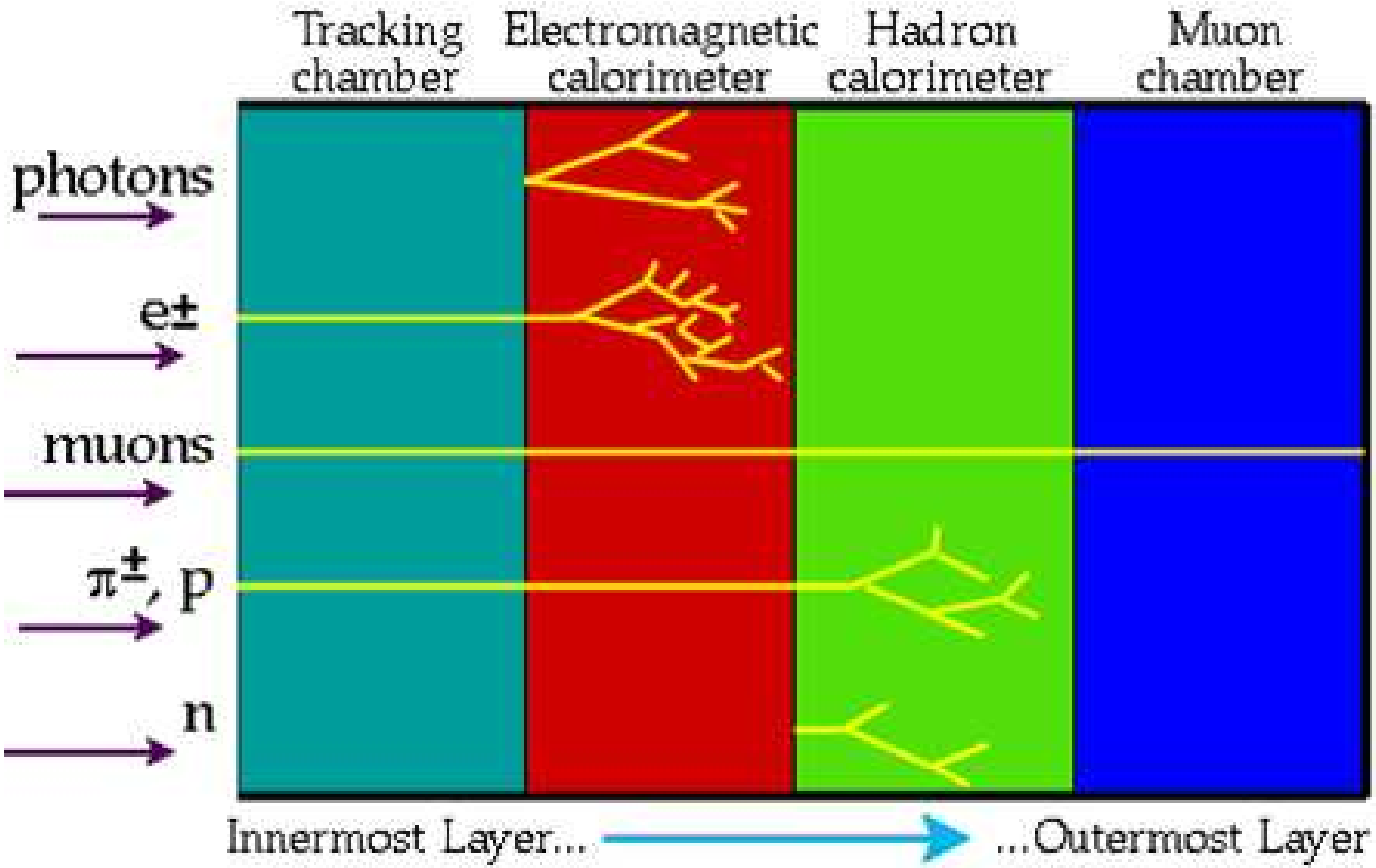

A closer look:

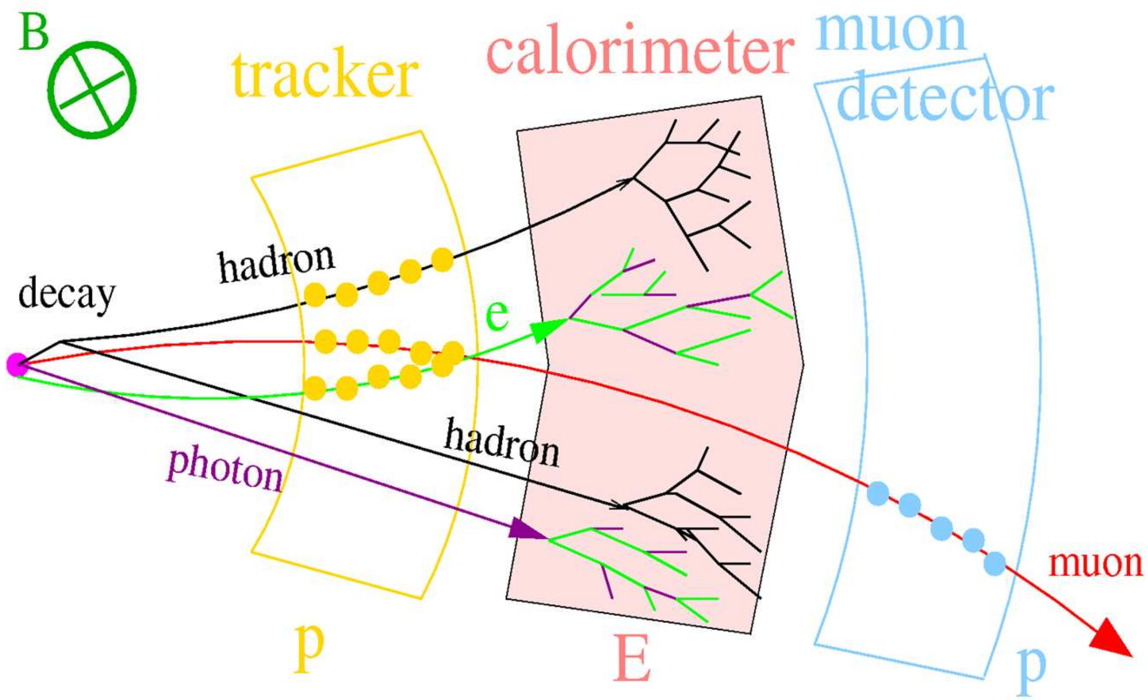

A closer look:

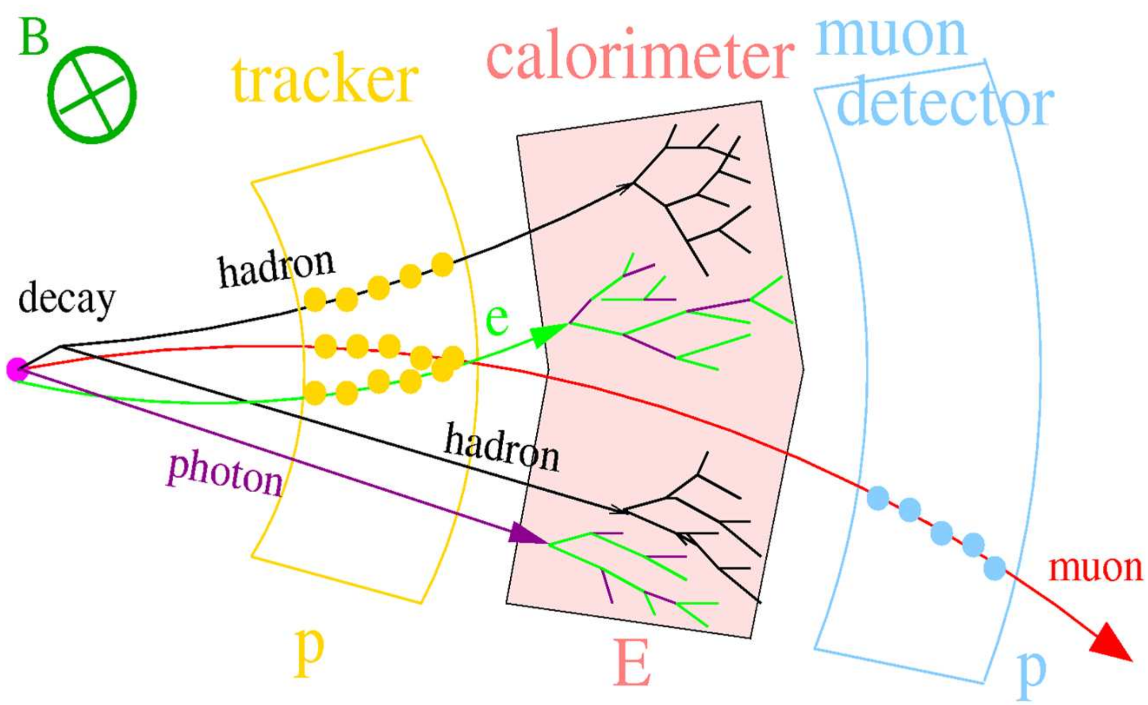

Theorists should know:

$$\text{For charged tracks}: \quad \Delta p/p \;\propto\; p,$$
$$\text{typical resolution}: \quad \sim\; p/(10^4\ \text{GeV}).$$
$$\text{For calorimetry}: \quad \Delta E/E \;\propto\; \frac{1}{\sqrt{E}},$$
$$\text{typical resolution}: \quad \sim\; (5-80\%)/\sqrt{E/\text{GeV}}.$$

† For vertex-tagged particles $\tau \approx 10^{-12}$ s,
heavy flavor tagging: the secondary vertex:

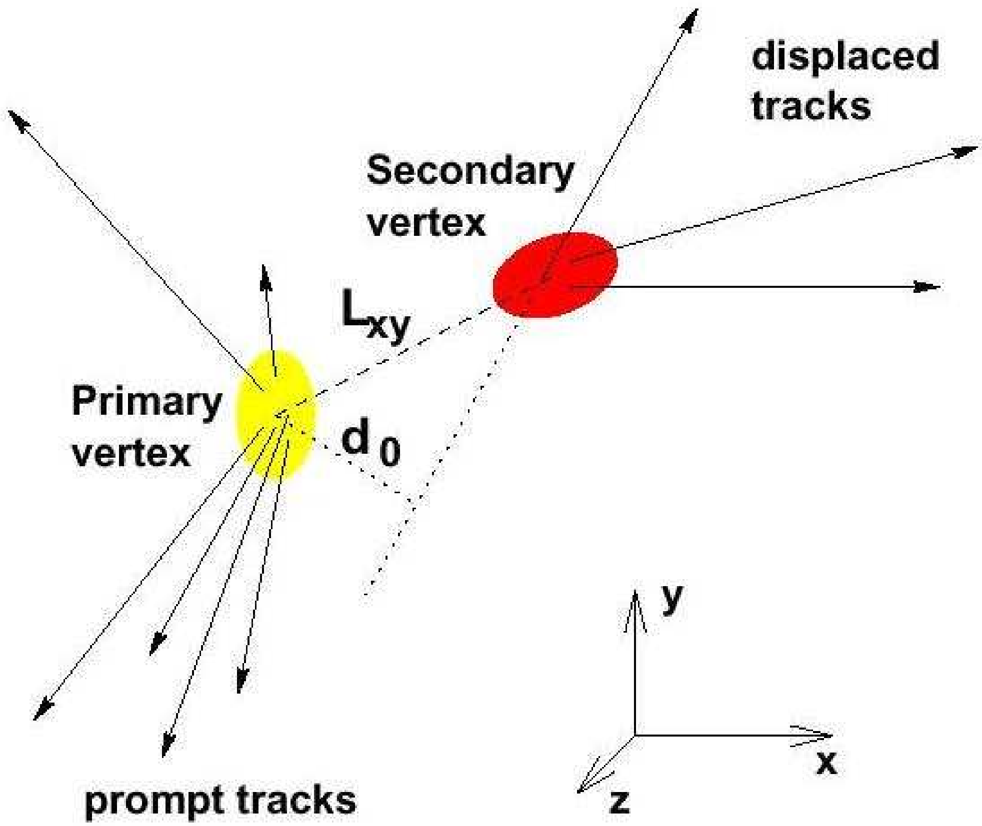

† For vertex-tagged particles $\tau \approx 10^{-12}$ s,
heavy flavor tagging: the secondary vertex:

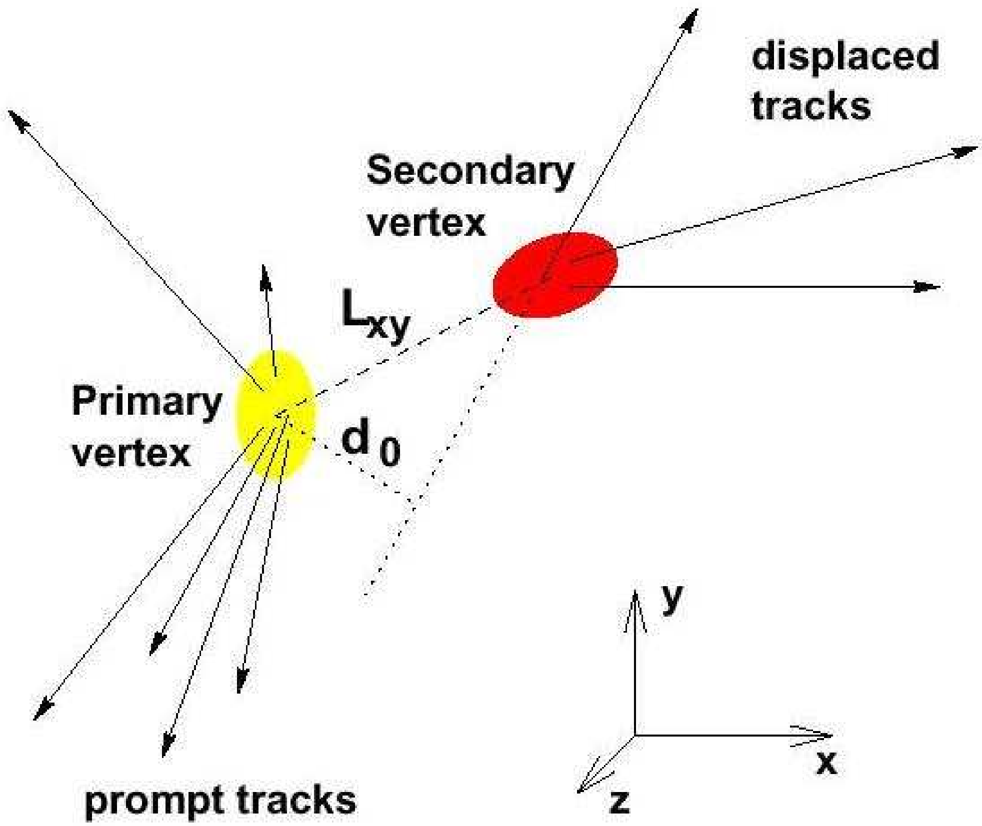

Typical resolution: $d_0 \sim 30 - 50\ \mu$m or so

$\Rightarrow$ Better have two (non-collinear) charged tracks for a secondary vertex;

Or use the "impact parameter" w.r.t. the primary vertex.

For theorists: just multiply a "tagging efficiency" $\epsilon_b \sim 40 - 60\%$ or so.

† For short-lived particles: $\tau < 10^{-12}$ s or so,
make use of final state kinematics to reconstruct the resonance.

† For short-lived particles: $\tau < 10^{-12}$ s or so,
make use of final state kinematics to reconstruct the resonance.

† For missing particles:
make use of energy-momentum conservation to deduce their existence.

$$p_1^i + p_2^i = \sum_f^{obs.} p_f + p_{miss}.$$

† For short-lived particles: $\tau < 10^{-12}$ s or so,
make use of final state kinematics to reconstruct the resonance.

† For missing particles:
make use of energy-momentum conservation to deduce their existence.

$$p_1^i + p_2^i = \sum_f^{obs.} p_f + p_{miss}.$$

But in hadron collisions, the longitudinal momenta unkown,
thus transverse direction only:

$$0 = \sum_f^{obs.} \vec{p}_{f\ T} + \vec{p}_{miss\ T}.$$

often called "missing p_T" ($\not{p}_T$) or "missing E_T" ($\not{E}_T$).

What we "see" for the SM particles
(no universality – sorry!)

Leptons	Vetexing	Tracking	ECAL	HCAL	Muon Cham.
$e^\pm$	$\times$	$\vec{p}$	E	$\times$	$\times$
$\mu^\pm$	$\times$	$\vec{p}$	$\surd$	$\surd$	$\vec{p}$
$\tau^\pm$	$\surd\times$	$\surd$	$e^\pm$	$h^\pm$; $3h^\pm$	$\mu^\pm$
ν_e, ν_μ, ν_τ	$\times$	$\times$	$\times$	$\times$	$\times$
Quarks					
u, d, s	$\times$	$\surd$	$\surd$	$\surd$	$\times$
$c \longrightarrow D$	$\surd$	$\surd$	$e^\pm$	h's	$\mu^\pm$
$b \longrightarrow B$	$\surd$	$\surd$	$e^\pm$	h's	$\mu^\pm$
$t \longrightarrow bW^\pm$	b	$\surd$	$e^\pm$	$b +$ 2 jets	$\mu^\pm$
Gauge bosons					
γ	$\times$	$\times$	E	$\times$	$\times$
g	$\times$	$\surd$	$\surd$	$\surd$	$\times$
$W^\pm \longrightarrow \ell^\pm \nu$	$\times$	$\vec{p}$	$e^\pm$	$\times$	$\mu^\pm$
$\longrightarrow q\bar{q}'$	$\times$	$\surd$	$\surd$	2 jets	$\times$
$Z^0 \longrightarrow \ell^+\ell^-$	$\times$	$\vec{p}$	$e^\pm$	$\times$	$\mu^\pm$
$\longrightarrow q\bar{q}$	$(b\bar{b})$	$\surd$	$\surd$	2 jets	$\times$

How to search for new particles?

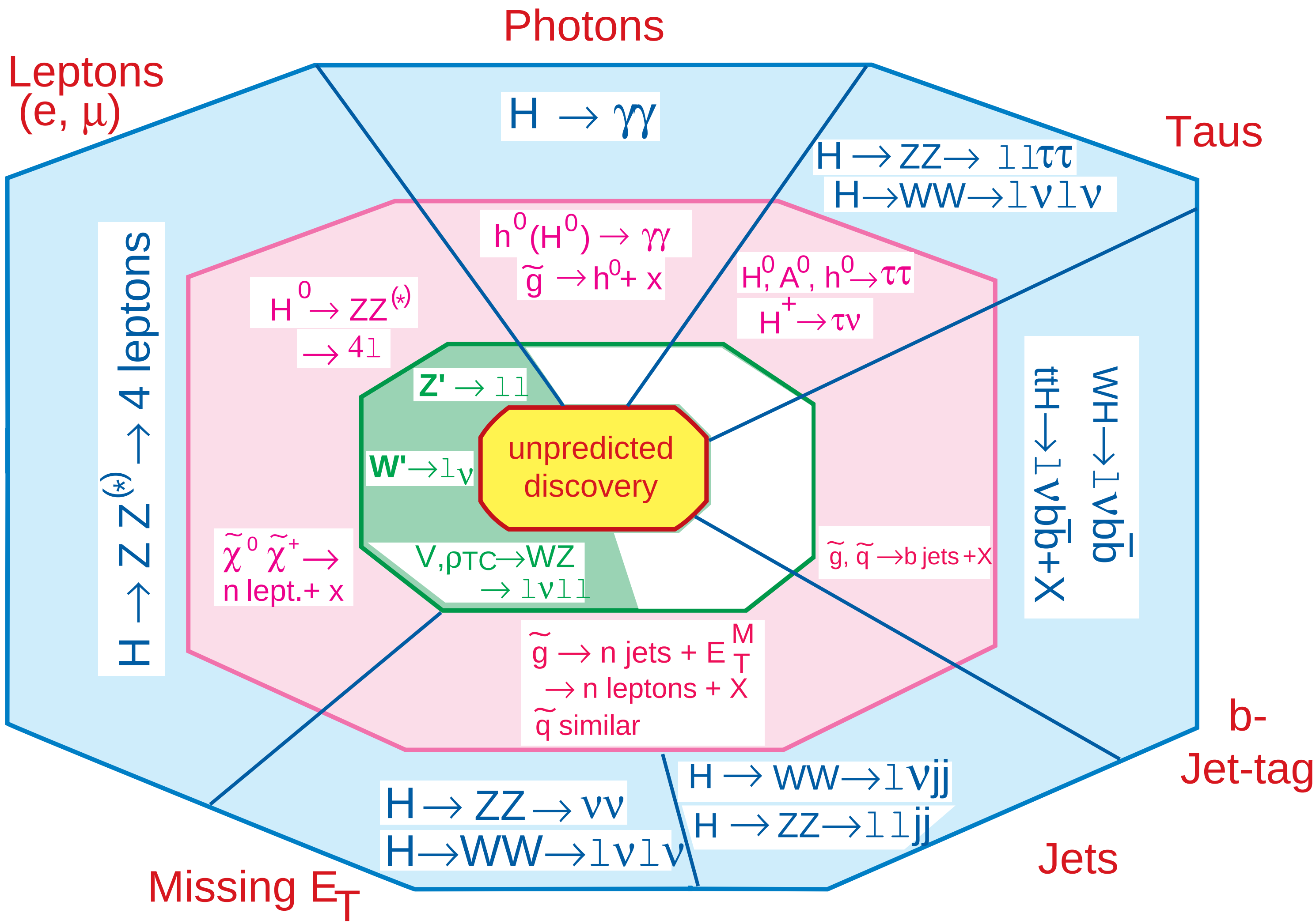

y98014_416dPauss rd

Homework:

Exercise 1.1: For a π^0, μ^-, or a τ^- respectively, calculate its decay length for $E = 10$ GeV.

Exercise 1.2: An event was identified to have a $\mu^+\mu^-$ pair, along with some missing energy. What can you say about the kinematics of the system of the missing particles? Consider both an e^+e^- and a hadron collider.

Exercise 1.3: Electron and muon measurements: Estimate the relative errors of energy-momentum measurements for an electron by an electromagnetic calorimetry ($\Delta E/E$) and for a muon by tracking ($\Delta p/p$) at energies of $E = 50$ GeV and 500 GeV, respectively.

Exercise 1.4: A 120 GeV Higgs boson will have a production cross section of 20 pb at the LHC. How many events per year do you expect to produce for the Higgs boson with an instantaneous luminosity $10^{33}/\text{cm}^2/\text{s}$? Do you expect it to be easy to observe and why?

II. Basic Techniques and Tools for Collider Physics

(A). Scattering cross section

For a $2 \to n$ scattering process:

$$\sigma(ab \to 1+2+...n) = \frac{1}{2s}\ \overline{\sum}|\mathcal{M}|^2\ dPS_n,$$

$$dPS_n \equiv (2\pi)^4\ \delta^4\left(P - \sum_{i=1}^{n} p_i\right) \Pi_{i=1}^{n} \frac{1}{(2\pi)^3}\frac{d^3\vec{p}_i}{2E_i},$$

$$s = (p_a + p_b)^2 \equiv P^2 = \left(\sum_{i=1}^{n} p_i\right)^2,$$

where $\overline{\sum}|\mathcal{M}|^2$: dynamics (dimension $4 - 2n$);

dPS_n: kinematics (Lorentz invariant, dimension $2n - 4.$)

II. Basic Techniques and Tools for Collider Physics

(A). Scattering cross section

For a $2 \to n$ scattering process:

$$\sigma(ab \to 1+2+...n) = \frac{1}{2s} \overline{\sum} |\mathcal{M}|^2 \, dPS_n,$$

$$dPS_n \equiv (2\pi)^4 \, \delta^4 \left(P - \sum_{i=1}^{n} p_i \right) \Pi_{i=1}^{n} \frac{1}{(2\pi)^3} \frac{d^3\vec{p}_i}{2E_i},$$

$$s = (p_a + p_b)^2 \equiv P^2 = \left(\sum_{i=1}^{n} p_i \right)^2,$$

where $\overline{\sum} |\mathcal{M}|^2$: dynamics (dimension $4-2n$);

dPS_n: kinematics (Lorentz invariant, dimension $2n-4$.)

For a $1 \to n$ decay process, the partial width in the rest frame:

$$\Gamma(a \to 1+2+...n) = \frac{1}{2M_a} \overline{\sum} |\mathcal{M}|^2 \, dPS_n.$$

$$\tau = \Gamma_{tot}^{-1} = (\sum_f \Gamma_f)^{-1}.$$

(B). Phase space and kinematics *

One-particle Final State $a + b \to 1$:

$$
\begin{aligned}
dPS_1 &\equiv (2\pi)\,\frac{d^3\vec{p}_1}{2E_1}\delta^4(P - p_1) \\
&\doteq \pi|\vec{p}_1|d\Omega_1\delta^3(\vec{P} - \vec{p}_1) \\
&\doteq 2\pi\ \delta(s - m_1^2).
\end{aligned}
$$

where the first and second equal signs made use of the identities:

$$
|\vec{p}|d|\vec{p}| = EdE, \quad \frac{d^3\vec{p}}{2E} = \int d^4p\ \delta(p^2 - m^2).
$$

*E.Byckling, K. Kajantie: Particle Kinemaitcs (1973).

(B). Phase space and kinematics *

One-particle Final State $a + b \to 1$:

$$
\begin{aligned}
dPS_1 &\equiv (2\pi)\ \frac{d^3\vec{p}_1}{2E_1}\delta^4(P - p_1) \\
&\doteq \pi|\vec{p}_1|d\Omega_1\delta^3(\vec{P} - \vec{p}_1) \\
&\doteq 2\pi\ \delta(s - m_1^2).
\end{aligned}
$$

where the first and second equal signs made use of the identities:

$$
|\vec{p}|d|\vec{p}| = EdE, \quad \frac{d^3\vec{p}}{2E} = \int d^4p\ \delta(p^2 - m^2).
$$

Kinematical relations:

$$
\begin{aligned}
\vec{P} &\equiv \vec{p}_a + \vec{p}_b = \vec{p}_1, \quad E_1^{cm} = \sqrt{s} \text{ in the c.m. frame,} \\
s &= (p_a + p_b)^2 = m_1^2.
\end{aligned}
$$

*E.Byckling, K. Kajantie: Particle Kinemaitcs (1973).

(B). Phase space and kinematics *

One-particle Final State $a+b\to 1$:

$$dPS_1 \equiv (2\pi)\,\frac{d^3\vec{p}_1}{2E_1}\delta^4(P-p_1)$$
$$\doteq \pi|\vec{p}_1|d\Omega_1\delta^3(\vec{P}-\vec{p}_1)$$
$$\doteq 2\pi\ \delta(s-m_1^2).$$

where the first and second equal signs made use of the identities:

$$|\vec{p}|d|\vec{p}| = EdE, \quad \frac{d^3\vec{p}}{2E} = \int d^4p\ \delta(p^2-m^2).$$

Kinematical relations:

$$\vec{P} \equiv \vec{p}_a+\vec{p}_b=\vec{p}_1, \quad E_1^{cm}=\sqrt{s} \text{ in the c.m. frame,}$$
$$s = (p_a+p_b)^2=m_1^2.$$

The "dimensinless phase-space volume" is $s(dPS_1)=2\pi$.

*E.Byckling, K. Kajantie: Particle Kinemaitcs (1973).

Two-particle Final State $a+b \to 1+2$:

$$\begin{aligned}
dPS_2 &\equiv \frac{1}{(2\pi)^2}\,\delta^4\left(P-p_1-p_2\right)\frac{d^3\vec{p}_1}{2E_1}\frac{d^3\vec{p}_2}{2E_2} \\
&\doteq \frac{1}{(4\pi)^2}\,\frac{|\vec{p}_1^{\,cm}|}{\sqrt{s}}\,d\Omega_1 = \frac{1}{(4\pi)^2}\,\frac{|\vec{p}_1^{\,cm}|}{\sqrt{s}}\,d\cos\theta_1 d\phi_1 \\
&= \frac{1}{4\pi}\frac{1}{2}\,\lambda^{1/2}\left(1,\frac{m_1^2}{s},\frac{m_2^2}{s}\right)dx_1 dx_2, \\
d\cos\theta_1 &= 2dx_1, \quad d\phi_1 = 2\pi dx_2, \quad 0 \le x_{1,2} \le 1,
\end{aligned}$$

Two-particle Final State $a + b \to 1 + 2$:

$$\begin{aligned}
dPS_2 &\equiv \frac{1}{(2\pi)^2}\ \delta^4(P - p_1 - p_2)\,\frac{d^3\vec{p}_1}{2E_1}\frac{d^3\vec{p}_2}{2E_2} \\
&\doteq \frac{1}{(4\pi)^2}\ \frac{|\vec{p}_1^{\,cm}|}{\sqrt{s}}\ d\Omega_1 = \frac{1}{(4\pi)^2}\ \frac{|\vec{p}_1^{\,cm}|}{\sqrt{s}}\ d\cos\theta_1 d\phi_1 \\
&= \frac{1}{4\pi}\frac{1}{2}\ \lambda^{1/2}\left(1, \frac{m_1^2}{s}, \frac{m_2^2}{s}\right) dx_1 dx_2, \\
d\cos\theta_1 &= 2dx_1, \quad d\phi_1 = 2\pi dx_2, \quad 0 \le x_{1,2} \le 1,
\end{aligned}$$

The magnitudes of the energy-momentum of the two particles are fully determined by the four-momentum conservation:

$$|\vec{p}_1^{\,cm}| = |\vec{p}_2^{\,cm}| = \frac{\lambda^{1/2}(s, m_1^2, m_2^2)}{2\sqrt{s}},\ \ E_1^{cm} = \frac{s + m_1^2 - m_2^2}{2\sqrt{s}},\ \ E_2^{cm} = \frac{s + m_2^2 - m_1^2}{2\sqrt{s}},$$

$$\lambda(x, y, z) = (x - y - z)^2 - 4yz = x^2 + y^2 + z^2 - 2xy - 2xz - 2yz.$$

Two-particle Final State $a + b \to 1 + 2$:

$$
\begin{aligned}
dPS_2 &\equiv \frac{1}{(2\pi)^2}\,\delta^4(P - p_1 - p_2)\,\frac{d^3\vec{p}_1}{2E_1}\frac{d^3\vec{p}_2}{2E_2} \\
&\doteq \frac{1}{(4\pi)^2}\,\frac{|\vec{p}_1^{\,cm}|}{\sqrt{s}}\,d\Omega_1 = \frac{1}{(4\pi)^2}\,\frac{|\vec{p}_1^{\,cm}|}{\sqrt{s}}\,d\cos\theta_1 d\phi_1 \\
&= \frac{1}{4\pi}\frac{1}{2}\,\lambda^{1/2}\left(1, \frac{m_1^2}{s}, \frac{m_2^2}{s}\right) dx_1 dx_2, \\
d\cos\theta_1 &= 2dx_1, \quad d\phi_1 = 2\pi dx_2, \quad 0 \le x_{1,2} \le 1,
\end{aligned}
$$

The magnitudes of the energy-momentum of the two particles are fully determined by the four-momentum conservation:

$$
|\vec{p}_1^{\,cm}| = |\vec{p}_2^{\,cm}| = \frac{\lambda^{1/2}(s, m_1^2, m_2^2)}{2\sqrt{s}}, \;\; E_1^{cm} = \frac{s + m_1^2 - m_2^2}{2\sqrt{s}}, \;\; E_2^{cm} = \frac{s + m_2^2 - m_1^2}{2\sqrt{s}},
$$

$$
\lambda(x, y, z) = (x - y - z)^2 - 4yz = x^2 + y^2 + z^2 - 2xy - 2xz - 2yz.
$$

The phase-space volume of the two-body is scaled down with respect to that of the one-particle by a factor

$$
\frac{dPS_2}{s\ dPS_1} \approx \frac{1}{(4\pi)^2}.
$$

just like a “loop factor”.

Consider a 2 $\rightarrow$ 2 scattering process $p_a + p_b \rightarrow p_1 + p_2$,

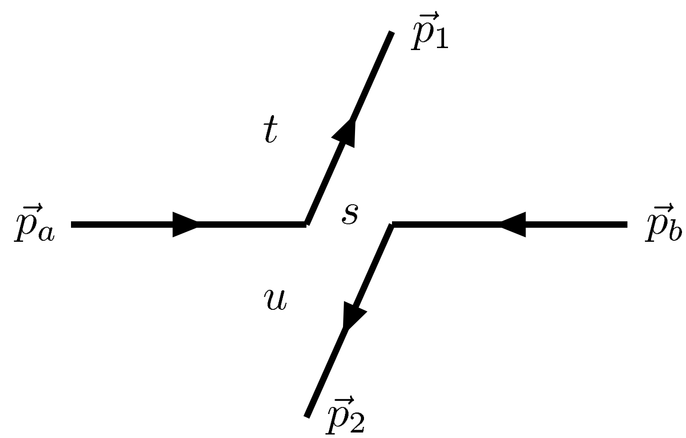

the (Lorentz invariant) Mandelstam variables are defined as

$$
\begin{aligned}
s &= (p_a + p_b)^2 = (p_1 + p_2)^2 = E_{cm}^2, \\
t &= (p_a - p_1)^2 = (p_b - p_2)^2 = m_a^2 + m_1^2 - 2(E_a E_1 - p_a p_1 \cos\theta_{a1}), \\
u &= (p_a - p_2)^2 = (p_b - p_1)^2 = m_a^2 + m_2^2 - 2(E_a E_2 - p_a p_2 \cos\theta_{a2}), \\
& s + t + u = m_a^2 + m_b^2 + m_1^2 + m_2^2.
\end{aligned}
$$

Consider a $2 \to 2$ scattering process $p_a + p_b \to p_1 + p_2$,

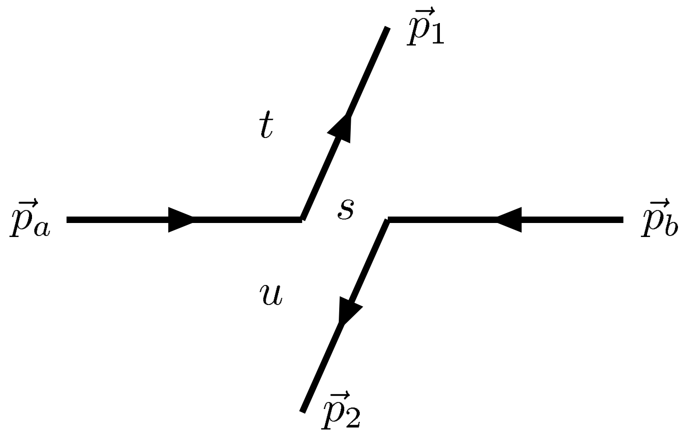

the (Lorentz invariant) Mandelstam variables are defined as

$$\begin{aligned} s &= (p_a + p_b)^2 = (p_1 + p_2)^2 = E_{cm}^2, \\ t &= (p_a - p_1)^2 = (p_b - p_2)^2 = m_a^2 + m_1^2 - 2(E_a E_1 - p_a p_1 \cos\theta_{a1}), \\ u &= (p_a - p_2)^2 = (p_b - p_1)^2 = m_a^2 + m_2^2 - 2(E_a E_2 - p_a p_2 \cos\theta_{a2}), \\ & s + t + u = m_a^2 + m_b^2 + m_1^2 + m_2^2. \end{aligned}$$

The two-body phase space can be thus written as

$$dPS_2 = \frac{1}{(4\pi)^2} \, \frac{dt \ d\phi_1}{s \ \lambda^{1/2}\left(1, m_a^2/s, m_b^2/s\right)}.$$

Exercise 2.1: Assume that $m_a = m_1$ and $m_b = m_2$. Show that

$$\begin{aligned} t &= -2p_{cm}^2(1 - \cos\theta^*_{a1}), \\ u &= -2p_{cm}^2(1 + \cos\theta^*_{a1}) + \frac{(m_1^2 - m_2^2)^2}{s}, \end{aligned}$$

$p_{cm} = \lambda^{1/2}(s, m_1^2, m_2^2)/2\sqrt{s}$ is the momentum magnitude in the c.m. frame.
Note: t is negative-definite; $t \to 0$ in the collinear limit.

Exercise 2.2: A particle of mass M decays to two particles isotropically in its rest frame. What does the momentum distribution look like in a frame in which the particle is moving with a speed β_z? Compare the result with your expectation for the shape change for a basket ball.

Three-particle Final State $a + b \to 1 + 2 + 3$:

$$
\begin{aligned}
dPS_3 &\equiv \frac{1}{(2\pi)^5}\,\delta^4(P - p_1 - p_2 - p_3)\,\frac{d^3\vec{p}_1}{2E_1}\frac{d^3\vec{p}_2}{2E_2}\frac{d^3\vec{p}_3}{2E_3} \\
&\doteq \frac{|\vec{p}_1|^2\ d|\vec{p}_1|\ d\Omega_1}{(2\pi)^3\ 2E_1}\ \frac{1}{(4\pi)^2}\ \frac{|\vec{p}_2^{(23)}|}{m_{23}}\ d\Omega_2 \\
&= \frac{1}{(4\pi)^3}\ \lambda^{1/2}\left(1, \frac{m_2^2}{m_{23}^2}, \frac{m_3^2}{m_{23}^2}\right)\ 2|\vec{p}_1|\ dE_1\ dx_2dx_3dx_4dx_5.
\end{aligned}
$$

$$
\begin{aligned}
d\cos\theta_{1,2} &= 2dx_{2,4}, \quad d\phi_{1,2} = 2\pi dx_{3,5}, \quad 0 \le x_{2,3,4,5} \le 1, \\
& |\vec{p}_1^{cm}|^2 = |\vec{p}_2^{cm} + \vec{p}_3^{cm}|^2 = (E_1^{cm})^2 - m_1^2, \\
& m_{23}^2 = s - 2\sqrt{s}E_1^{cm} + m_1^2, \quad |\vec{p}_2^{23}| = |\vec{p}_3^{23}| = \frac{\lambda^{1/2}(m_{23}^2, m_2^2, m_3^2)}{2m_{23}},
\end{aligned}
$$

Three-particle Final State $a + b \to 1 + 2 + 3$:

$$
\begin{aligned}
dPS_3 &\equiv \frac{1}{(2\pi)^5}\, \delta^4(P - p_1 - p_2 - p_3) \frac{d^3\vec{p}_1}{2E_1}\frac{d^3\vec{p}_2}{2E_2}\frac{d^3\vec{p}_3}{2E_3} \\
&\doteq \frac{|\vec{p}_1|^2 \; d|\vec{p}_1| \; d\Omega_1}{(2\pi)^3 \; 2E_1} \frac{1}{(4\pi)^2} \frac{|\vec{p}_2^{(23)}|}{m_{23}} \, d\Omega_2 \\
&= \frac{1}{(4\pi)^3} \, \lambda^{1/2}\left(1, \frac{m_2^2}{m_{23}^2}, \frac{m_3^2}{m_{23}^2}\right) \; 2|\vec{p}_1| \; dE_1 \; dx_2 dx_3 dx_4 dx_5.
\end{aligned}
$$

$$
\begin{aligned}
d\cos\theta_{1,2} &= 2dx_{2,4}, \quad d\phi_{1,2} = 2\pi dx_{3,5}, \quad 0 \le x_{2,3,4,5} \le 1, \\
& |\vec{p}_1^{cm}|^2 = |\vec{p}_2^{cm} + \vec{p}_3^{cm}|^2 = (E_1^{cm})^2 - m_1^2, \\
& m_{23}^2 = s - 2\sqrt{s}E_1^{cm} + m_1^2, \quad |\vec{p}_2^{23}| = |\vec{p}_3^{23}| = \frac{\lambda^{1/2}(m_{23}^2, m_2^2, m_3^2)}{2m_{23}},
\end{aligned}
$$

The particle energy spectrum is not monochromatic.
The maximum value (the end-point) for particle 1 in c.m. frame is

$$
\begin{aligned}
E_1^{max} &= \frac{s + m_1^2 - (m_2 + m_3)^2}{2\sqrt{s}}, \quad m_1 \le E_1 \le E_1^{max}, \\
|\vec{p}_1^{max}| &= \frac{\lambda^{1/2}(s, m_1^2, (m_2 + m_3)^2)}{2\sqrt{s}}, \quad 0 \le p_1 \le p_1^{max}.
\end{aligned}
$$

With $m_i = 10,\ 20,\ 30,\ \sqrt{s} = 100$ GeV.

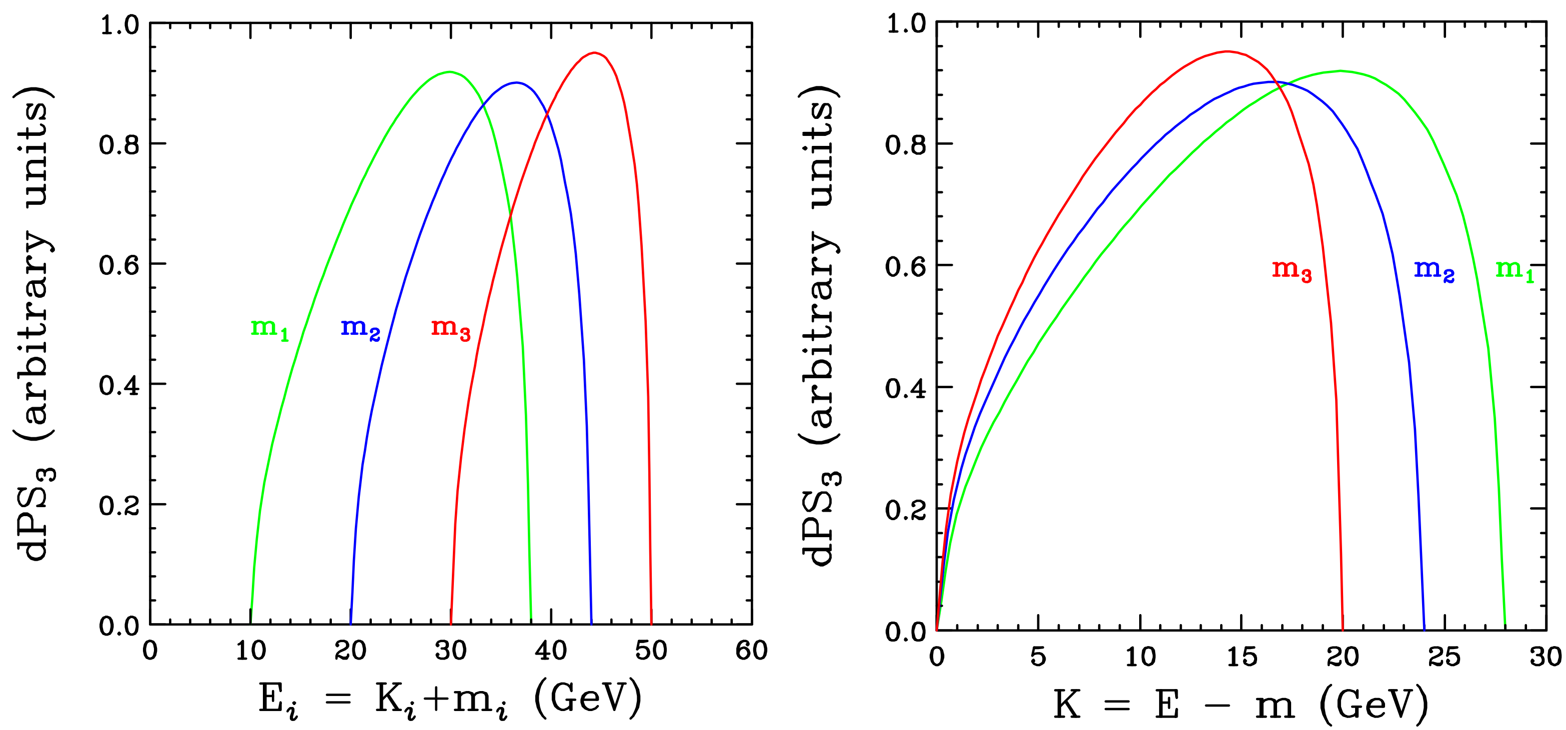

More intuitive to work out the end-point for the kinetic energy,
– recall the direct neutrino mass bound in β-decay:

$$K_1^{max} = E_1^{max} - m_1 = \frac{(\sqrt{s} - m_1 - m_2 - m_3)(\sqrt{s} - m_1 + m_2 + m_3)}{2\sqrt{s}}.$$

In general, the 3-body phase space boundaries are non-trivial.
That leads to the "Dalitz Plots".

One practically useful formula is:

Exercise 2.3: A particle of mass M decays to 3 particles $M \to abc$.
Show that the phase space element can be expressed as

$$dPS_3 = \frac{1}{2^7\pi^3}\ M^2 dx_a dx_b.$$

$$x_i = \frac{2E_i}{M},\ \ (i = a, b, c,\ \sum_i x_i = 2).$$

where the integration limits for $m_a = m_b = m_c = 0$ are

$$0 \le x_a \le 1, \quad 1 - x_a \le x_b \le 1.$$

Recursion relation $P \to 1 + 2 + 3 ... + n$:

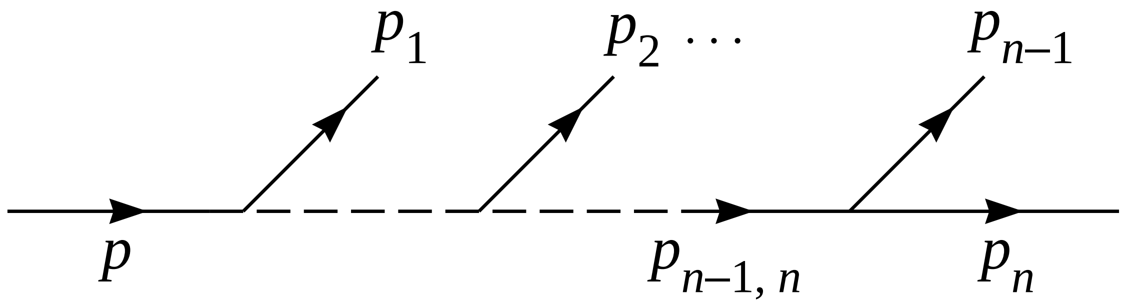

Recursion relation $P \to 1 + 2 + 3 ... + n$:

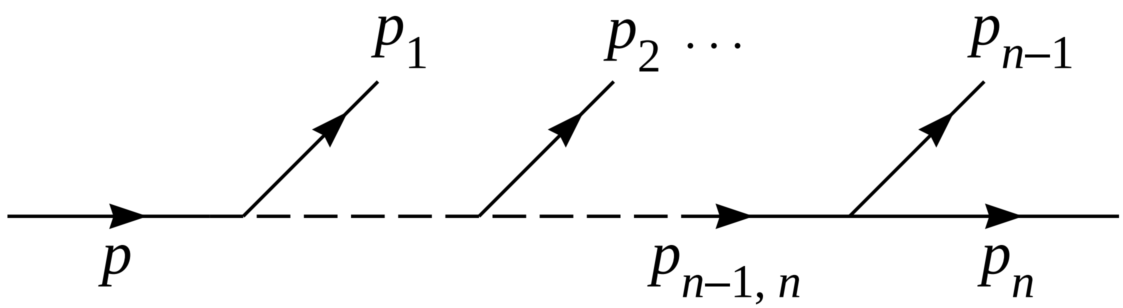

$$dPS_n(P; p_1, ..., p_n) = dPS_{n-1}(P; p_1, ..., p_{n-1,n})$$
$$dPS_2(p_{n-1,n}; p_{n-1}, p_n)\frac{dm^2_{n-1,n}}{2\pi}.$$

For instance,

$$dPS_3 = dPS_2(i)\ \frac{dm^2_{prop}}{2\pi}\ dPS_2(f).$$

This is generically true, but particularly useful when the diagram has an s-channel particle propagation.

Breit-Wigner Resonance, the Narrow Width Approximation

An unstable particle of mass M and total width Γ_V, the propagator is

$$R(s) = \frac{1}{(s - M_V^2)^2 + \Gamma_V^2 M_V^2}.$$

Consider an intermediate state V^*

$$a \to bV^* \to b\ p_1 p_2.$$

By the reduction formula, the resonant integral reads

$$\int_{(m_*^{min})^2=(m_1+m_2)^2}^{(m_*^{max})^2=(m_a-m_b)^2} dm_*^2.$$

Variable change

$$\tan\theta = \frac{m_*^2 - M_V^2}{\Gamma_V M_V},$$

resulting in a flat integrand over θ

$$\int_{(m_*^{min})^2}^{(m_*^{max})^2} \frac{dm_*^2}{(m_*^2 - M_V^2)^2 + \Gamma_V^2 M_V^2} = \int_{\theta^{min}}^{\theta^{max}} \frac{d\theta}{\Gamma_V M_V}.$$

In the limit

$$(m_1 + m_2) + \Gamma_V \ll M_V \ll m_a - \Gamma_V,$$
$$\theta^{min} = \tan^{-1} \frac{(m_1 + m_2)^2 - M_V^2}{\Gamma_V M_V} \to -\pi,$$
$$\theta^{max} = \tan^{-1} \frac{(m_a - m_b)^2 - M_V^2}{\Gamma_V M_V} \to 0,$$

then the Narrow Width Approximation

$$\frac{1}{(m_*^2 - M_V^2)^2 + \Gamma_V^2 M_V^2} \approx \frac{\pi}{\Gamma_V M_V}\ \delta(m_*^2 - M_V^2).$$

In the limit

$$
\begin{aligned}
(m_1+m_2)+\Gamma_V \ll M_V \ll m_a-\Gamma_V,\\
\theta^{min} = \tan^{-1}\frac{(m_1+m_2)^2-M_V^2}{\Gamma_V M_V} \to -\pi,\\
\theta^{max} = \tan^{-1}\frac{(m_a-m_b)^2-M_V^2}{\Gamma_V M_V} \to 0,
\end{aligned}
$$

then the Narrow Width Approximation

$$\frac{1}{(m_*^2-M_V^2)^2+\Gamma_V^2 M_V^2} \approx \frac{\pi}{\Gamma_V M_V}\ \delta(m_*^2-M_V^2).$$

Exercise 2.4: Consider a three-body decay of a top quark, $t \to bW^* \to b\ e\nu$. Making use of the phase space recursion relation and the narrow width approximation for the intermediate W boson, show that the partial decay width of the top quark can be expressed as

$$\Gamma(t \to bW^* \to b\ e\nu) \approx \Gamma(t\to bW)\cdot BR(W\to e\nu).$$

(C). Matrix element: The dynamics

Properties of scattering amplitudes

(C). Matrix element: The dynamics
Properties of scattering amplitudes

• Analyticity: A scattering amplitude is analytical except:
simple poles (corresponding to single particle states, bound states etc.);
branch cuts (corresponding to thresholds).

(C). Matrix element: The dynamics

Properties of scattering amplitudes

• Analyticity: A scattering amplitude is analytical except:
simple poles (corresponding to single particle states, bound states etc.);
branch cuts (corresponding to thresholds).

• Crossing symmetry: A scattering amplitude for a $2 \to 2$ process is symmetric among the s-, t-, u-channels.

(C). Matrix element: The dynamics

Properties of scattering amplitudes

- Analyticity: A scattering amplitude is analytical except:

simple poles (corresponding to single particle states, bound states etc.); branch cuts (corresponding to thresholds).

- Crossing symmetry: A scattering amplitude for a $2 \to 2$ process is symmetric among the s-, t-, u-channels.

- Unitarity:

S-matrix unitarity leads to :

$$-i(T - T^\dagger) = TT^\dagger$$

Partial wave expansion for $a + b \to 1 + 2$:

$$\mathcal{M}(s,t) = 16\pi \sum_{J=M}^{\infty} (2J+1) a_J(s) d^J_{\mu\mu'}(\cos\theta)$$

$$a_J(s) = \frac{1}{32\pi} \int_{-1}^{1} \mathcal{M}(s,t)\ d^J_{\mu\mu'}(\cos\theta) d\cos\theta.$$

where $\mu = s_a - s_b,\ \mu' = s_1 - s_2,\ J = \max(|\mu|, |\mu'|)$.

Partial wave expansion for $a + b \to 1 + 2$:

$$\begin{aligned} \mathcal{M}(s,t) &= 16\pi \sum_{J=M}^{\infty} (2J+1) a_J(s) d^J_{\mu\mu'}(\cos\theta) \\ a_J(s) &= \frac{1}{32\pi} \int_{-1}^{1} \mathcal{M}(s,t)\ d^J_{\mu\mu'}(\cos\theta) d\cos\theta. \end{aligned}$$

where $\mu = s_a - s_b,\ \mu' = s_1 - s_2,\ J = \max(|\mu|, |\mu'|)$.

By Optical Theorem: $\sigma = \frac{1}{s} \mathrm{Im} \mathcal{M}(\theta = 0) = \frac{16\pi}{s} \sum_{J=M}^{\infty} (2J+1) |a_J(s)|^2$.

Partial wave expansion for $a+b\to 1+2$:

$$\mathcal{M}(s,t) = 16\pi \sum_{J=M}^{\infty}(2J+1)a_J(s)d^J_{\mu\mu'}(\cos\theta)$$
$$a_J(s) = \frac{1}{32\pi}\int_{-1}^{1}\mathcal{M}(s,t)\; d^J_{\mu\mu'}(\cos\theta)d\cos\theta.$$

where $\mu = s_a - s_b,\ \mu' = s_1 - s_2,\ J = \max(|\mu|,|\mu'|)$.

By Optical Theorem: $\sigma = \frac{1}{s}\mathrm{Im}\mathcal{M}(\theta=0) = \frac{16\pi}{s}\sum_{J=M}^{\infty}(2J+1)|a_J(s)|^2$.

The partial wave amplitude have the properties:

(a). partial wave unitarity: $\mathrm{Im}(a_J)\geq |a_J|^2$, or $|\mathrm{Re}(a_J)|\leq 1/2$,

(b). kinematical thresholds: $a_J(s)\propto \beta_i^{l_i}\ \beta_f^{l_f}\ \ (J=L+S)$.

Partial wave expansion for $a + b \to 1 + 2$:

$$\mathcal{M}(s,t) = 16\pi \sum_{J=M}^{\infty} (2J+1) a_J(s) d^J_{\mu\mu'}(\cos\theta)$$

$$a_J(s) = \frac{1}{32\pi} \int_{-1}^{1} \mathcal{M}(s,t)\ d^J_{\mu\mu'}(\cos\theta) d\cos\theta.$$

where $\mu = s_a - s_b,\ \mu' = s_1 - s_2,\ J = \max(|\mu|, |\mu'|)$.

By Optical Theorem: $\sigma = \frac{1}{s}\mathrm{Im}\mathcal{M}(\theta = 0) = \frac{16\pi}{s}\sum_{J=M}^{\infty}(2J+1)|a_J(s)|^2$.

The partial wave amplitude have the properties:

(a). partial wave unitarity: $\mathrm{Im}(a_J) \geq |a_J|^2$, or $|\mathrm{Re}(a_J)| \leq 1/2$,

(b). kinematical thresholds: $a_J(s) \propto \beta_i^{l_i}\ \beta_f^{l_f}\quad (J = L + S)$.

$\Rightarrow$ well-known behavior: $\sigma \propto \beta_f^{2l_f+1}$.

Partial wave expansion for $a+b\to 1+2$:

$$\begin{aligned}\mathcal{M}(s,t) &= 16\pi\sum_{J=M}^{\infty}(2J+1)a_J(s)d^J_{\mu\mu'}(\cos\theta)\\ a_J(s) &= \frac{1}{32\pi}\int_{-1}^{1}\mathcal{M}(s,t)\ d^J_{\mu\mu'}(\cos\theta)d\cos\theta.\end{aligned}$$

where $\mu=s_a-s_b,\ \mu'=s_1-s_2,\ J=\max(|\mu|,|\mu'|)$.

By Optical Theorem: $\sigma=\frac{1}{s}\mathrm{Im}\mathcal{M}(\theta=0)=\frac{16\pi}{s}\sum_{J=M}^{\infty}(2J+1)|a_J(s)|^2$.

The partial wave amplitude have the properties:

(a). partial wave unitarity: $\mathrm{Im}(a_J)\ge|a_J|^2$, or $|\mathrm{Re}(a_J)|\le 1/2$,

(b). kinematical thresholds: $a_J(s)\propto\beta_i^{l_i}\ \beta_f^{l_f}\quad(J=L+S)$.

$\Rightarrow$ well-known behavior: $\sigma\propto\beta_f^{2l_f+1}$.

Exercise 2.5: Appreciate the properties (a) and (b) by explicitly calculating the helicity amplitudes for

$$e^-_Le^+_R\to\gamma^*\to H^-H^+,\quad e^-_Le^+_{L,R}\to\gamma^*\to\mu^-_L\mu^+_R,\quad H^-H^+\to G^*\to H^-H^+.$$

(D). Calculational Tools

Traditional "Trace" Techniques:

* You should be good at this — QFT course!

With algebraic symbolic manipulations:

* REDUCE
* FORM
* MATHEMATICA, MAPLE ...

(D). Calculational Tools

Traditional "Trace" Techniques:

∗ You should be good at this — QFT course!

With algebraic symbolic manipulations:

∗ REDUCE

∗ FORM

∗ MATHEMATICA, MAPLE ...

Helicity Techniques:

More suitable for direct numerical evaluations.

∗ Hagiwara-Zeppenfeld: best for massless particles... (NPB)

∗ CalCul Method (by T.T. Wu et al., Parke-Mangano: Phys. Report);

∗ New techniques in loop calculations
(by Z.Bern, L.Dixon, W. Giele, N. Glover, K.Melnikov, F. Petriello ...)

∗ "Twisters" (string theory motivated organization)
(by Britto, F.Chachazo, B.Feng, E.Witten ...)

(D). Calculational Tools

Traditional "Trace" Techniques:

* You should be good at this — QFT course!

With algebraic symbolic manipulations:

* REDUCE
* FORM
* MATHEMATICA, MAPLE ...

Helicity Techniques:

More suitable for direct numerical evaluations.

* Hagiwara-Zeppenfeld: best for massless particles... (NPB)
* CalCul Method (by T.T. Wu et al., Parke-Mangano: Phys. Report);
* New techniques in loop calculations
  (by Z.Bern, L.Dixon, W. Giele, N. Glover, K.Melnikov, F. Petriello ...)
* "Twisters" (string theory motivated organization)
  (by Britto, F.Chachazo, B.Feng, E.Witten ...)

Exercise 2.6: Calculate the squared matrix element for $\overline{\sum}|\mathcal{M}(f\bar{f}\to ZZ)|^2$, in terms of s, t, u, in whatever technique you like.

Calculational packages:

check up at http://www.ippp.dur.ac.uk/montecarlo/BSM

- Monte Carlo packages for phase space integration:

(1) VEGAS by P. LePage: adaptive important-sampling MC
http://en.wikipedia.org/wiki/Monte-Carlo_integration

(2) SAMPLE, RAINBOW, MISER ...

- Automated software for matrix elements:

(1) REDUCE — an interactive program designed for general algebraic computations, including to evaluate Dirac algebra, an old-time program,
http://www.uni-koeln.de/REDUCE;
http://reduce-algebra.com.

(2) FORM by Jos Vermaseren: A program for large scale symbolic manipulation, evaluate fermion traces automatically,
and perform loop calculations,s commercially available at
http://www.nikhef.nl/ form

(3) FeynCalc and FeynArts: Mathematica packages for algebraic calculations in elementary particle physics.
http://www.feyncalc.org;
http://www.feynarts.de

(4) MadGraph: Helicity amplitude method for tree-level matrix elements available upon request or
http://madgraph.hep.uiuc.edu

- Automated evaluation of cross sections:

(1) MadGraph/MadEvent and MadSUSY:
Generate Fortran codes on-line!
http://madgraph.hep.uiuc.edu

(2) CompHEP/CalHEP: computer program for calculation of elementary particle processes in Standard Model and beyond. CompHEP has a built-in numeric interpreter. So this version permits to make numeric calculation without additional Fortran/C compiler. It is convenient for more or less simple calculations.

— It allows your own construction of a Lagrangian model!

http://theory.npi.msu.su/~kryukov

(3) GRACE and GRACE SUSY: squared matrix elements (Japan)
http://minami-home.kek.jp

(4) AlpGen: higher-order tree-level SM matrix elements (M. Mangano ...):
http://mlm.home.cern.ch/mlm/alpgen/

(5) SHERPA (F. Krauss et al.):
Generate Fortran codes on-line! Merging with MC generators (see next).
http://www.sherpa-mc.de/

(6) Pandora by M. Peskin:
C++ based package for e^+e^-, including beam effects.
http://www-sldnt.slac.stanford.edu/nld/new/Docs/Generators/PANDORA.htm
The program pandora is a general-purpose parton-level event generator which includes beamstrahlung, initial state radiation, and full treatment of polarization effects. (An interface to PYTHIA that produces fully hadronized events is possible.)

- Cross sections at NLO packages:

MC(at)NLO (B. Webber et al.):
http://www.hep.phy.cam.ac.uk/theory/webber/MCatNLO/

• Numerical simulation packages:

(1) PYTHIA:

PYTHIA is a Monte Carlo program for the generation of high-energy physics events, i.e. for the description of collisions at high energies between e^+, e^-, p and $\bar{p}$ in various combinations.
They contain theory and models for a number of physics aspects, including hard and soft interactions, parton distributions, initial and final state parton showers, multiple interactions, fragmentation and decay.

— It can be combined with MadGraph and detector simulations.

http://www.thep.lu.se/ torbjorn/Pythia.html

• Numerical simulation packages:

(1) PYTHIA:

PYTHIA is a Monte Carlo program for the generation of high-energy physics events, i.e. for the description of collisions at high energies between e^+, e^-, p and $\bar{p}$ in various combinations.
They contain theory and models for a number of physics aspects, including hard and soft interactions, parton distributions, initial and final state parton showers, multiple interactions, fragmentation and decay.

— It can be combined with MadGraph and detector simulations.

http://www.thep.lu.se/ torbjorn/Pythia.html

(2) HERWIG

HERWIG is a Monte Carlo program which simulates $pp, p\bar{p}$ interactions at high energies. It has the most sophisticated perturbative treatments, and possible NLO QCD matrix elements in parton showing.

http://hepwww.rl.ac.uk/theory/seymour/herwig/

(3) ISAJET

ISAJET is a Monte Carlo program which simulates $pp, \bar{p}p$, and ee interactions at high energies. It is largely obsolete.

ISASUSY option is still useful.

http://www.phy.bnl.gov/ isajet

(3) ISAJET

ISAJET is a Monte Carlo program which simulates $pp, \bar{p}p$, and ee interactions at high energies. It is largely obsolete.

ISASUSY option is still useful.

http://www.phy.bnl.gov/ isajet

• "Pretty Good Simulation" (PGS):

By John Conway: A simplified detector simulation, mainly for theorists to estimate the detector effects.

http://www.physics.ucdavis.edu/ conway/research/software/pgs/pgs.html

PGS has been adopted for running with PYTHIA and MadGraph.